The anti-apoptotic role of Mcl-1 during early nervous system development

by © Robert T. Flemmer

A Thesis submitted to the School of Graduate Studies in partial fulfilment of the requirements for the degree of **Master of Science in Medicine (Neuroscience)**.

Division of BioMedical Sciences/Faculty of Medicine

Memorial University of Newfoundland

May 2019

St. John's Newfoundland and Labrador

Abstract

Developmental neurogenesis, the formation of neurons *in utero*, is tightly regulated by apoptosis, a form of programmed cell death. The pro-survival protein Mcl-1 has been shown to be important for the survival of the developing nervous system through its ability to inhibit apoptosis. This dependency is poorly understood. Moreover, how Mcl-1 inhibits apoptosis in the developing nervous system is unknown. Here, conditional ablation of *mcl-1* in the murine developing nervous system (Mcl-1 CKO) resulted in widespread death throughout the developing nervous system. Mcl-1 CKOs showed a progression of apoptosis that mirrors the progression of differentiation in the brainstem and spinal cord. Apoptosis was rescued by co-deleting pro-apoptotic Bax in Mcl-1 CKO mice, demonstrating that Mcl-1 promotes cell survival by blocking the activation of Bax. This work is the first to demonstrate widespread dependency on Mcl-1 during early nervous system development.

Acknowledgements

The work described in this thesis would not be possible were it not for the support and mentorship of my supervisor, Dr. Jacqueline Vanderluit. Her leadership and guidance have allowed me to prosper professionally and personally.

I would also like to thank Dr. Matthew Parsons and Dr. Ken Kao for their expert opinions and critical eyes and Ms. Katie Fifield for her training and support.

Lastly, I am indebted to the many faculty members, graduate students, support staff, friends and family who led me through my master's program. A sense of community is essential for one to thrive and my success is only through this sense of community.

Table of Contents

List of Tables

List of Figures

List of Abbreviations and Symbols

°C – degrees Celsius

% – percent

µg – micrograms

µl – microlitre

µm – micrometer

µM – micromolar

1X – one times

A1 – Bcl-2-related protein A1

AC3 – active Caspase 3

APAF 1 – Apoptotic protease activating factor 1

AU – arbitrary units

Bad – Bcl-2 associated death promotor

Bak – Bcl-2 homologous antagonist killer

Bax – Bcl-2-associated X protein

bax$^{(-/-)}$ – Bax Null

bax$^{(f/f)}$ – Bax Floxed

Bcl-2 – B cell lymphoma-2

Bcl-B – Bcl-2-like protein 10

Bcl-w – Bcl-2-like protein 2

Bcl-XL – B-cell lymphoma-extra large

BH – Bcl-2 homology

Bid – BH3 interacting

Bik – Bcl-2 interacting killer

Bim – Bcl-2-like protein 11

Bmf – Bcl-2-modifying factor

Bmp – Bone morphogenetic protein

BPB – bromophenol blue

BSA – bovine serum albumin

CARD – Caspase-recruitment domains

CO_2 – carbon dioxide

Complete IP buffer – complete immunoprecipitation buffer

Ctl – control

ddH_2O – double distilled water

DED – Death effector domains

E – Embryonic day

EDTA – Ethylenediaminetetraacetic acid

Fgf – Fibroblast growth factor

FIJI – Fiji is just ImageJ

H_2O – water

HET – heterozygous

Hrk – Harakiri

HRP – horse radish peroxidase

LIF – Leukemia Inhibitor Factor

Mcl-1 – Myeloid cell leukemia-1

Mcl-1 CKO – Mcl-1 conditional knock-out

mcl-1$^{(f/f)}$ – mcl-1 floxed

mg – milligram

min – minute

ml – millilitre

mM – millimolar

MOMP – Mitochondrial outer membrane permeabilization

nes:cre$^{+/-}$ – *nestin* mediated *cre*

nm – nanometer

nM – nanomolar

NPC – Neural precursor cells

P – postnatal day

Pen Strep – penicillin streptomycin

PEST – Proline, aspartic acid, serine, threonine

pH – power of hydrogen

PUMA – P53 upregulated modulator of apoptosis

RA – Retinoic acid

RGC – Radial glial cell

RPM – rotation per minute

SD – standard deviation

SDS-PAGE – sodium dodecyl sulfate polyacrylamide gel electrophoresis

Shh – Sonic hedgehog

SMAC – Second mitochondrial activator of Caspases

TAE – Tris-acetate EDTA

UV – ultraviolet

V – volts

v/v – volume per volume

w/v – weight per volume

Wnt – Wingless-related integration site

XIAP – X-linked inhibitor of apoptosis

1-0 Introduction

1-1 Overview of early formation of the nervous system

The complex tasks performed by the adult mammalian nervous system require many unique populations of cells, each with a specific locality, morphology, and gene expression profile. As such, developmental neurogenesis, the formation of the nervous system in an embryo, is tightly regulated to ensure proper postnatal functionality. The nervous system forms from the ectoderm shortly after gastrulation. Signaling from the notochord initiates the transformation of ectodermal cells to neuroectodermal cells. This results in a thickening known as the neural plate (Copp et al., 2003). In the mouse, neurulation, when the neural plate folds into the neural tube, begins at embryonic day 8 (E8) of the 21-day gestation period, although primitive neural stem cells are present at E5.5-E7.5 (Copp et al., 2003).

Neural stem cells are defined by three properties. First, they must be able to form neural tissue or be formed from neural tissue. Second, they must be able to self-renew, and third, they must be able to form other neural cells through asymmetric divisions (Gage, 2000). The early neural tube consists of Leukemia Inhibitory Factor (LIF)-responsive primitive neural stem cells, known as neuroepithelial cells, that divide symmetrically to form more neural stem cells (Hitoshi et al., 2004; Tropepe et al., 2001). These cells divide to form the definitive neural stem cells, known as radial glial cells (RGCs). RGCs are characterized by their expression of the intermediate filament protein Nestin beginning at E7.5 and their responsiveness to Fibroblast growth factor-2 (Fgf2) beginning at E8.5 (Hitoshi et al., 2004; Kawaguchi et al., 2001; Tropepe et al., 1999). The

definitive neural stem cells give rise to the astrocytes, neurons and oligodendrocytes that populate the brain and spinal cord (Ramasamy et al., 2013).

1-2 Developmental neurogenesis of the forebrain

The neocortex has served as the basic model for dorsal forebrain development. The cortex is comprised of six layers that form in an inside-out manner (Rakic, 1974). RGCs reside in the lumen of the neural tube that then becomes the ventricular zone but have processes that extend to the pial surface of the developing brain (Farkas & Huttner, 2008). RGCs divide symmetrically to produce two RGCs or two neurons, or asymmetrically to form an RGC and a cell committed to differentiate. It is in this manner that RGCs produce the post-mitotic neurons of the brain without extinguishing the progenitor population. The differentiating cells migrate and form the three main cell types of the brain: neurons, astrocytes and oligodendrocytes (Ohtaka-Maruyama & Okado, 2015).

Excitatory glutamatergic neurons migrate radially up the cortex, using the RGC's long processes to climb through the cortex. Inhibitory GABAergic neurons migrate tangentially from the ganglionic eminences to the cortex (Lavdas et al., 1999; Luhmann et al., 2015). The ganglionic eminences are a collection of three structures in the ventral telencephalon that protrude into the ventricular space (Figure 1-1). The lateral ganglionic eminence forms the striatum in the adult brain, and the medial ganglionic eminence forms pallidal structures in the adult brain and gives rise to cholinergic neurons. The caudal and medial ganglionic eminences produce the majority of cortical GABAergic interneurons (Turrero Garcia & Harwell, 2017). Neurogenesis in these regions varies, with

neurogenesis in the medial ganglionic eminence beginning at E9 and in the caudal ganglionic eminence at E12 (Miyoshi et al., 2007; Miyoshi et al., 2010).

The process by which neural stem cells and progenitor cells, collectively known as neural precursor cells (NPCs), proliferate and differentiate is highly controlled. Neurogenesis in the cerebral cortex of the mouse brain occurs over 11 successive cell divisions between E11 and E17 of the 21-day gestation period in mouse (Takahashi et al., 1995).

Figure 1-1. The ganglionic eminences shown through coronal sections of the developing telencephalon. **(A)** The lateral ganglionic eminence (pink) and the medial ganglionic eminence (yellow) develop in the E10 forebrain. **(B)** By E12, the caudal ganglionic eminence (blue) is formed. Both the medial and caudal ganglionic eminence produce GABAergic interneurons that migrate tangentially into the developing cortex (adapted from Turrero Garcia & Harwell, 2017).

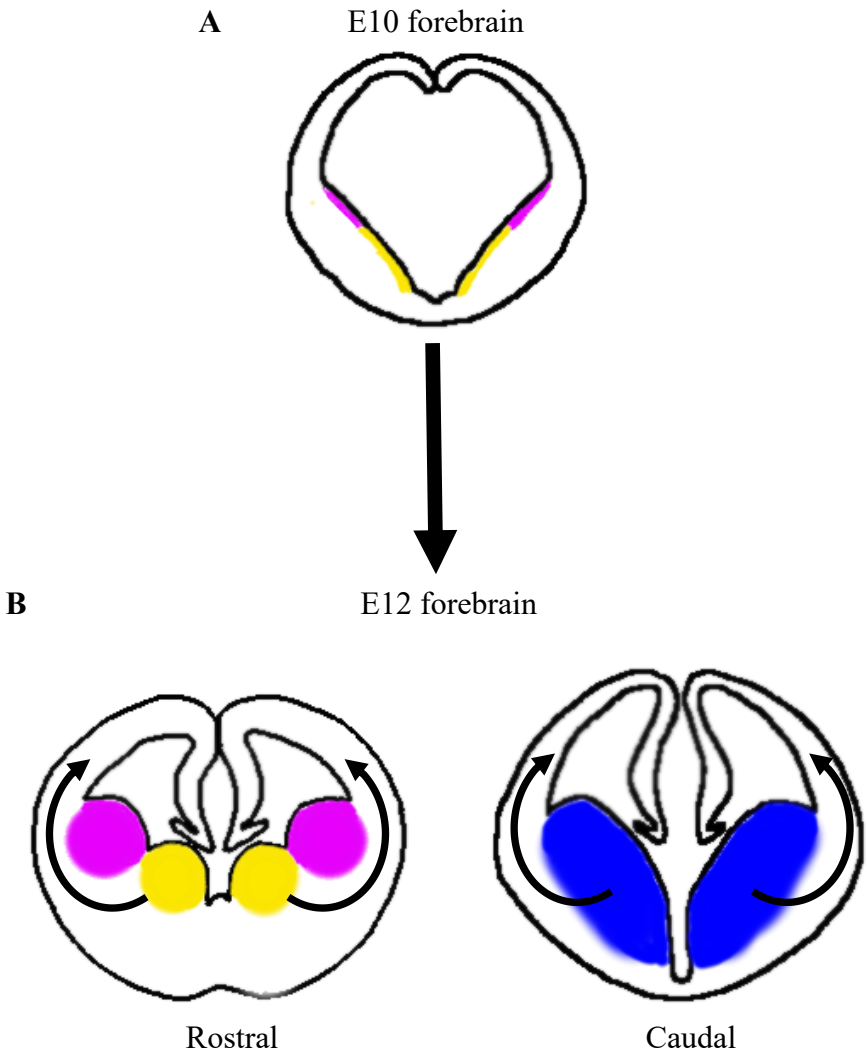
A
E10 forebrain
B
E12 forebrain
Rostral
Caudal

1-3 Developmental neurogenesis of the spinal cord

The patterning of the developing spinal cord is well characterized. Neurogenesis in the spinal cord begins at E9.5 and continues until E18.5 (Alaynick et al., 2011). The newly formed caudal neural tube becomes the spinal cord in the adult. As with the forebrain, development is tightly controlled, with several axes of development including rostral/caudal, dorsal/ventral and medial/lateral (Figure 1-2) (Gouti et al, 2015). The rostral/caudal axis is controlled caudally by gradients of Fgf8 and wingless-related integration site (Wnt), which maintain cells in a more stem-like state and cause the elongation of the spinal cord (Wilson et al., 2009). The rostral axis is controlled by gradients of retinoic acid (RA), which is secreted by the somites that line the developing neural tube and is associated with a reduction in body elongation (Olivera-Martinez et al., 2012). Exposure to RA causes cells to transition to a more lineage-restricted NPC fate (Gouti et al., 2015). On the dorsal/ventral axis, two opposing morphogen gradients cause the patterning of the spinal cord. The dorsal aspect of patterning is driven by gradients of bone morphogenetic protein (Bmp), whereas the ventral aspect is patterned by gradients of sonic hedgehog (Shh) (Simões-Costa & Bronner, 2015). These morphogens cause the expression of many different transcription factors along the dorsal/ventral axis that ultimately result in 12 unique regions (Gouti et al., 2015). The medial/lateral axis of the spinal cord varies based on state of differentiation, with the medial portion containing proliferating NPCs and the lateral portion containing differentiated cells. NPCs reside in the medial ventricular zone, which lines the central canal. As the NPCs differentiate, they migrate laterally (Ulloa & Briscoe, 2007). The proper formation of the spinal cord and

brain require regulation of cell numbers. A critical regulating feature is apoptosis, a type of programmed cell death.

Figure 1-2. Spinal cord neurogenesis is controlled by morphogen gradients in the dorsal/ventral, medial/lateral and rostral/caudal axes. **(A)** The rostral axis is controlled by gradients of RA and the caudal axis is controlled by gradients of Fgf and Wnt. Differentiation of NPCs begins in the rostral spinal cord and progresses caudally. **(B)** The dorsal axis is controlled by gradients of Bmp and the ventral axis is controlled by gradients of Shh. Differentiation of NPCs begins in the ventral spinal cord and progressing dorsally **(C)** As NPCs differentiate, they migrate laterally from the midline in the developing spinal cord.

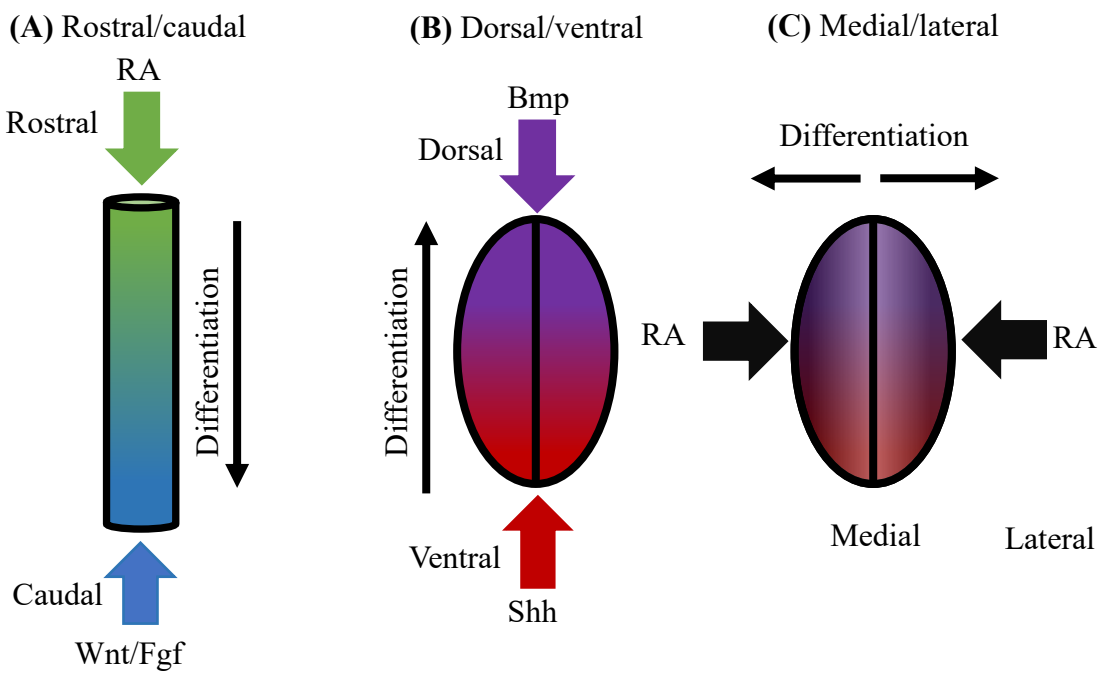
(A) Rostral/caudal
RA
Rostral
Differentiation
Caudal
Wnt/Fgf
(B) Dorsal/ventral
Bmp
Dorsal
Differentiation
Ventral
Shh
(C) Medial/lateral
Differentiation
RA
RA
Medial
Lateral

1-4 Apoptosis

The first identified form of regulated cell death was apoptosis. Apoptosis was originally classified based on the laddering of DNA and its morphology: shrinking of the cytoplasm, membrane blebbing, condensed nuclei, and nuclear fragmentation. Through a microscope, these apoptotic cells appear as small clusters of cell fragments (Kerr et al., 1972). There are two main signals by which apoptosis is activated: extrinsic signals and intrinsic signals. The extrinsic apoptotic pathway is activated via external environmental cues through specific death receptor activation on the surface of the cell, whereas intrinsic apoptosis results from intracellular stresses that do not activate the death receptors responsible for extrinsic apoptosis (Galluzzi et al., 2018). Both pathways converge on the activation of caspases. Although the result of both the extrinsic and intrinsic apoptotic pathways is the same, the process by which the cell gets to the final executioner caspase activation is different. The intrinsic apoptotic pathway plays a key role in the developing nervous system (Yuan & Yankner, 2000); therefore, for the purposes of this thesis, intrinsic apoptosis will be described in depth.

1-4-1 Caspases

Caspases are a family of cysteine-aspartic acid proteases normally found residing in an inactive form, where they are known as pro-Caspases. Three varieties of caspases exist, inflammatory caspases, initiator caspases and executioner caspases. Initiator and executioner caspases are responsible for the amplification and execution of the apoptotic cascade, respectively (Shalini et al., 2015). Initiator caspases such as Caspase 8 and 9

contain Death Effector Domains (DEDs) or Caspase-Recruitment Domains (CARDs) that are used to form complexes with other proteins that cleave and activate these caspases. Once activated, initiator caspases cleave and activate the executioner caspases such as Caspase 3 and 7, which are responsible for the dismantling of the cell (Thornberry & Lazebnik, 1998). The activation of Caspase 3 and Caspase 7 is the last step of the intrinsic apoptotic pathway. Caspase 3 activation is essential for apoptosis and results in DNA fragmentation, nuclear condensation and the proteolysis of many protein targets. Caspase 7 has few proteolytic targets and has a minor role in apoptosis compared to Caspase 3, though it is essential for cell detachment (Slee et al., 2001; Walsh et al., 2008; Brentnall et al., 2013). In combination with nuclear condensation, activation of Caspase 3 (AC3) is considered a marker for apoptosis (Boatright & Salvesen, 2003).

1-4-2 The mechanism of intrinsic apoptosis

Intrinsic apoptosis can result from several different stress signals such as DNA damage, growth factor deprivation and cell cycle arrest (Galluzzi et al., 2018). The central mechanism behind intrinsic apoptosis is mitochondrial outer membrane permeabilization (MOMP). MOMP serves two purposes in cell death. Firstly, MOMP causes a loss in mitochondrial membrane potential, leading to a loss in energy production. Secondly, MOMP results in the release of cytochrome c from the mitochondrial intermembrane space (Liu et al., 1996). Once released into the cytosol, cytochrome c binds apoptotic protease activating factor 1 (APAF 1) and pro-Caspase 9, to form a structure known as the apoptosome (Li et al., 1997). This apoptosome cleaves pro-

Caspase 9 into active Caspase 9, which in turn activates the executioner Caspase 3 and Caspase 7 (Li et al., 1997). Also released during MOMP are pro-apoptotic second mitochondrial activator of caspases (SMAC; also known as Diablo) (Du et al., 2000; Verhagen et al., 2000) and anti-apoptotic x-linked inhibitor of apoptosis (XIAP) (Roy et al., 1997). XIAP prevents apoptosis through the inhibition of Caspase activity and has been shown to inhibit apoptosis due to UV light exposure, chemotaxic drugs and activation of tumour necrosis factor (Duckett et al., 1998; Eckelman et al, 2006). SMAC promotes apoptosis through direct inhibition of XIAP (Du et al., 2000)

1-4-3 Apoptosis in the developing nervous system

Apoptosis is essential for proper nervous system development. In the central and peripheral nervous system, up to 50% of cells die of apoptosis (Dekkers et al., 2013). Prenatally, apoptosis occurs during neural tube closure, in the developing hindbrain, optic invaginations and proliferating precursor populations of the cortex. Apoptosis also occurs as post-mitotic neurons form synaptic connections (Copp et al., 2003; Yeo & Gautier, 2004). Apoptotic cell death continues postnatally in many cell populations, including the neocortex, hippocampus and brainstem (White & Barone, 2001). From initiation to clearance, apoptosis occurs on a time scale of a few hours (Bursch et al., 1990); therefore, despite the amount of apoptosis that occurs in the nervous system, the rapid progression means that only 2-3% of cells are undergoing apoptosis at any one point in time (White & Barone, 2001).

1-5 The Bcl-2 family of proteins

In the intrinsic apoptotic pathway, whether a cell lives or undergoes apoptosis is determined by the B cell lymphoma-2 (Bcl-2) family of proteins. This family of proteins is named after the founding member, Bcl-2, a potent anti-apoptotic protein (Tsujimoto et al., 1985; Vaux et al., 1988). The Bcl-2 family is characterized by Bcl-2 Homology (BH) domains. These domains interact with each other, and these interactions result in the activation or repression of the pro-apoptotic and anti-apoptotic properties of the Bcl-2 family (Youle & Strasser, 2008). There are three main categories of Bcl-2 family members: anti-apoptotic, pro-apoptotic BH3-only and pro-apoptotic effector proteins (Figure 1-3).

Figure 1-3. The Bcl-2 family of proteins. Diagrams of Bcl-2 family members demonstrating the BH1-4 domains they contain. Anti-apoptotic proteins oppose the activity of pro-apoptotic effector proteins, sensitizers and direct-activators. Many of the Bcl-2 family members have the ability to interact with membranes throughout the cell through their transmembrane (TM) domains (adapted from Giménez-Cassina & Danial, 2015).

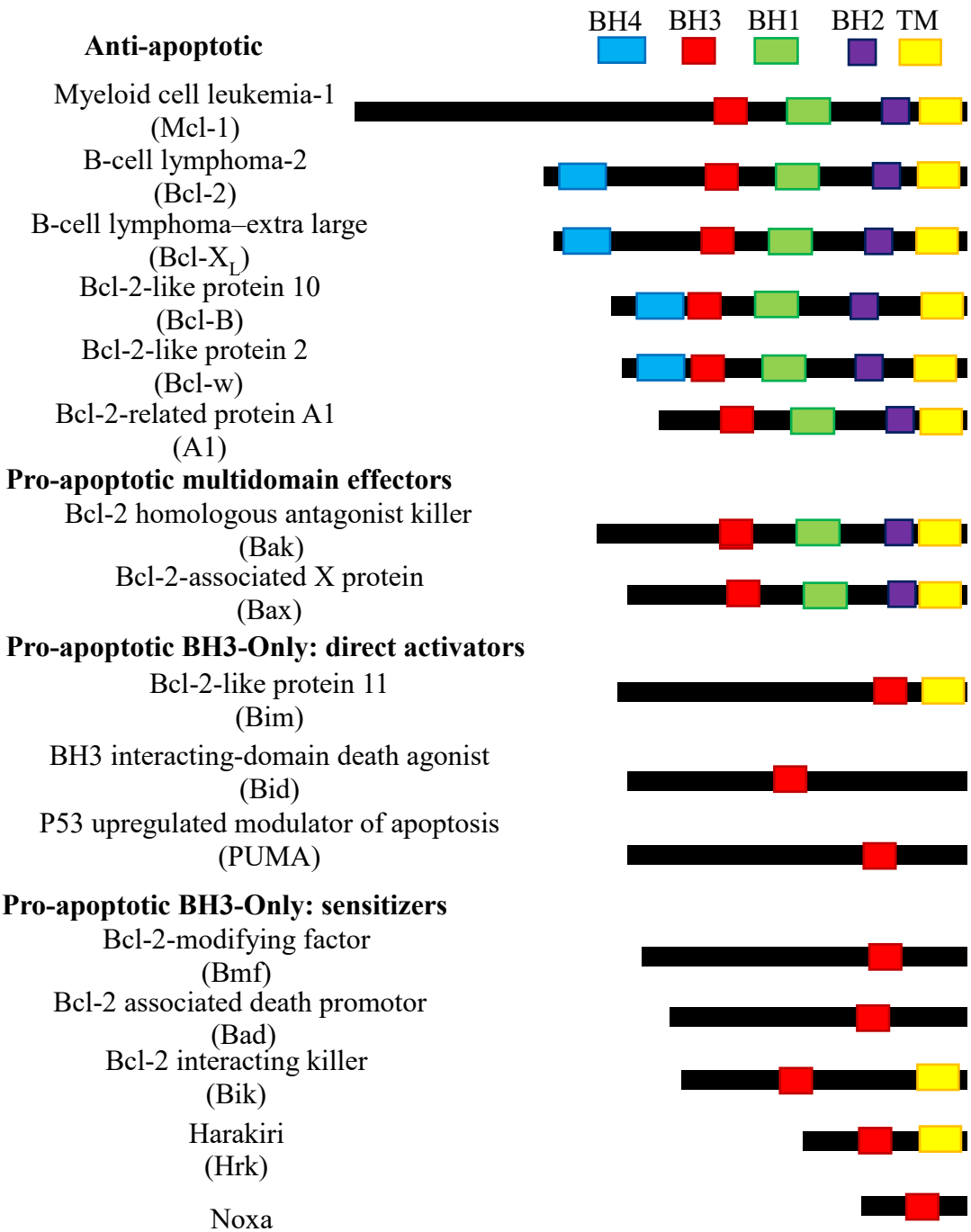
BH4
BH3
BH1
BH2
TM
Anti-apoptotic
Myeloid cell leukemia-1
(Mcl-1)
B-cell lymphoma-2
(Bcl-2)
B-cell lymphoma–extra large
(Bcl-X_L)
Bcl-2-like protein 10
(Bcl-B)
Bcl-2-like protein 2
(Bcl-w)
Bcl-2-related protein A1
(A1)
Pro-apoptotic multidomain effectors
Bcl-2 homologous antagonist killer
(Bak)
Bcl-2-associated X protein
(Bax)
Pro-apoptotic BH3-Only: direct activators
Bcl-2-like protein 11
(Bim)
BH3 interacting-domain death agonist
(Bid)
P53 upregulated modulator of apoptosis
(PUMA)
Pro-apoptotic BH3-Only: sensitizers
Bcl-2-modifying factor
(Bmf)
Bcl-2 associated death promotor
(Bad)
Bcl-2 interacting killer
(Bik)
Harakiri
(Hrk)
Noxa

The pro-apoptotic BH3-only proteins act as sensors throughout the cell, each specializing in the detection of different death signals. Two types of BH3-only proteins exist, direct activators and sensitizers. Direct activators such as Bim can directly activate the pro-apoptotic effector proteins (Gavathiotis et al., 2010). Sensitizers like Noxa function to displace and free direct activators that have been sequestered by anti-apoptotic proteins (Figure 1-4) (Willis et al., 2007).

Effector proteins, Bax and Bak, are responsible for forming multimer complexes with themselves that form pores in the mitochondrial outer membrane (Chittenden et al., 1995; Oltval et al., 1993). These are the pores through which cytochrome c enters the cytosol to continue the intrinsic apoptotic cascade. These effector proteins are activated by direct activator BH3-only proteins. The anti-apoptotic proteins bind both BH3-only and effector proteins to prevent apoptosis from occurring. An outline of the intrinsic apoptotic cascade can be seen in Figure 1-5 (Youle & Strasser, 2008).

Members of the Bcl-2 family show both selectivity and redundancy in their propensity to bind each other. The BH3-only direct activator proteins PUMA, Bid, and Bim bind anti-apoptotic proteins Bcl-2, Bcl-X_L, Mcl-1 and Bcl-w promiscuously. Bad binds Bcl-2, Bcl-X_L and Bcl-w, but not Mcl-1. Noxa is specific for Mcl-1 (Chen et al., 2005). Pro-apoptotic effector protein Bax has been shown to bind all anti-apoptotic proteins, whereas Bak has been shown to bind Bcl-X_L, Mcl-1 and A1 (Czabotar et al., 2014). BH3-only direct activator proteins such as Bid and Bim bind Bax and Bak directly, whereas sensitizers such as Bad do not bind Bax and Bak directly (Letai et al., 2002). A summary of interactions is diagramed in Figure 1-6.

Figure 1-4. BH3-only proteins can act as sensitizers or direct-activators. Direct-activators are inhibited by the anti-apoptotic Bcl-2 family members and activate Bax/Bak. Sensitizers inhibit the anti-apoptotic Bcl-2 members from inhibiting direct-activators or effector proteins (adapted from Green & Llambi, 2015).

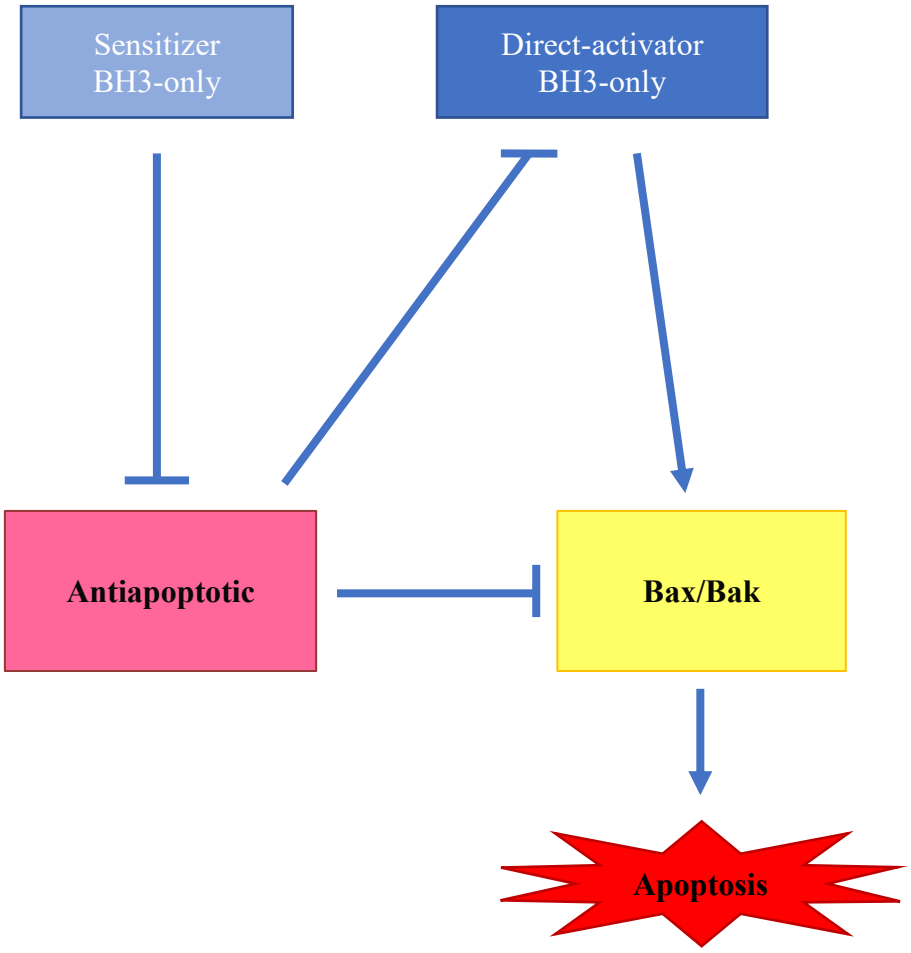
Sensitizer
BH3-only
Direct-activator
BH3-only
Antiapoptotic
Bax/Bak
Apoptosis

Figure 1-5. The intrinsic apoptotic pathway. Intracellular stresses activate the pro-apoptotic BH3-only proteins. In turn, the BH3-only proteins activate Bax/Bak, resulting in MOMP. Anti-apoptotic Bcl-2 family members such as Mcl-1 inhibit both BH3-only proteins and Bax/Bak. The release of cytochrome c and APAF-1 causes the formation of the apoptosome, which activates Caspase-9, which in turn, activates Caspase 3 to dismantle the cell (adapted from Youle & Strasser, 2008).

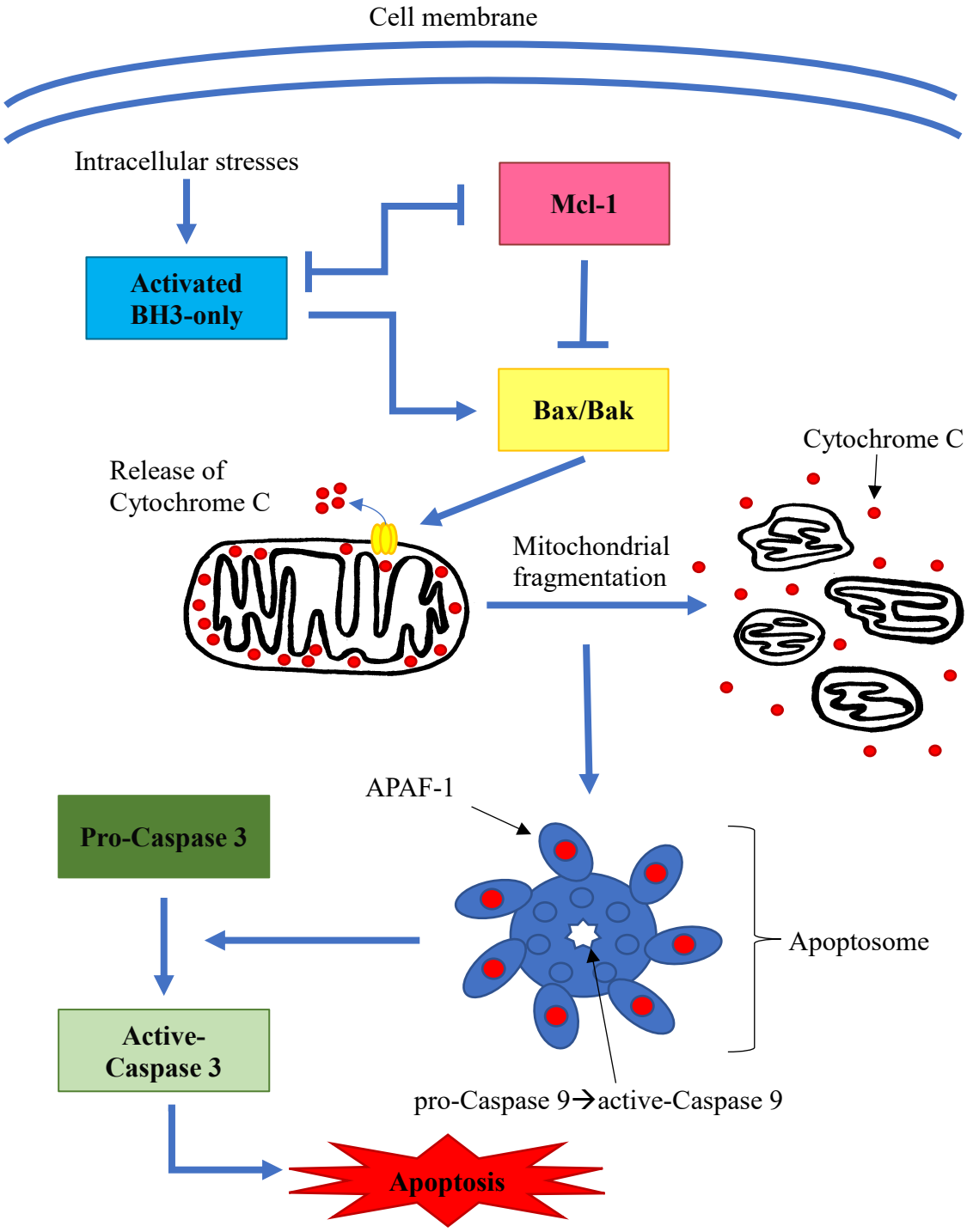
Cell membrane
Intracellular stresses
Mcl-1
Activated BH3-only
Bax/Bak
Release of Cytochrome C
Cytochrome C
Mitochondrial fragmentation
APAF-1
Pro-Caspase 3
Apoptosome
Active-Caspase 3
pro-Caspase 9→active-Caspase 9
Apoptosis

Figure 1-6. Interactions between the pro-apoptotic and anti-apoptotic Bcl-2 family members. Mcl-1 has been shown to interact with pro-apoptotic effector proteins Bax and Bak, BH3-only sensitizers (light blue) and BH3-only direct activators (dark blue) (adapted from Czabotar et al., 2014; Moldoveanu et al., 2014).

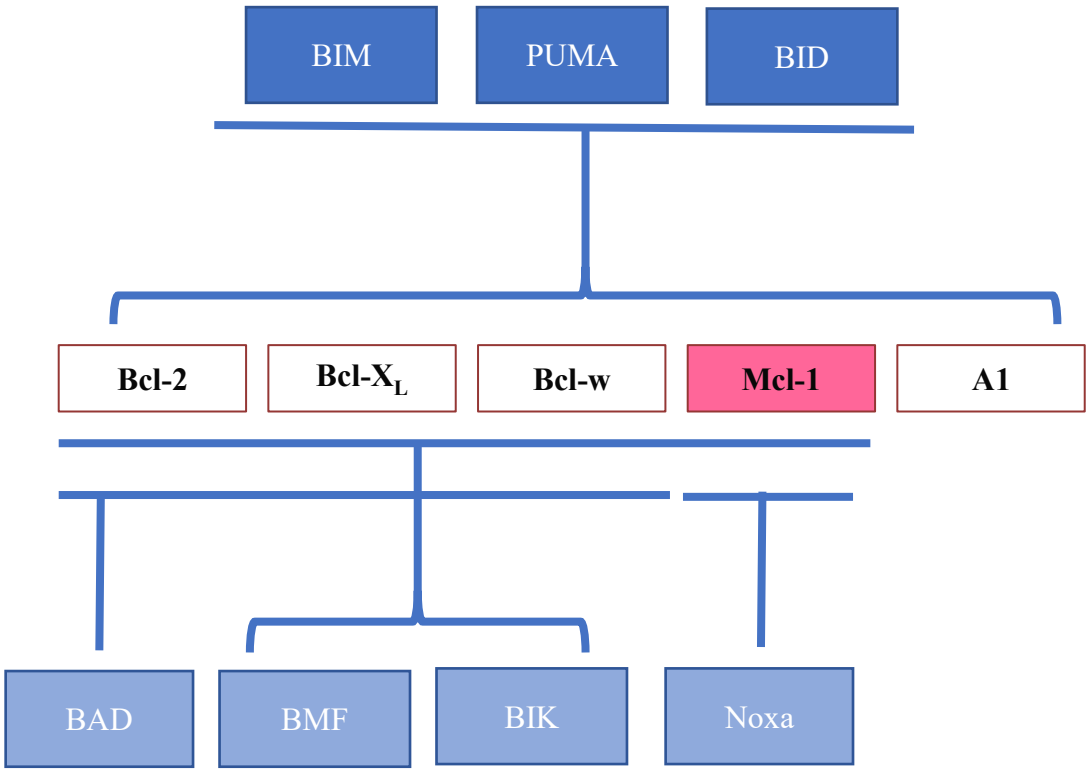
BIM
PUMA
BID
Bcl-2
Bcl-X$_L$
Bcl-w
Mcl-1
A1
BAD
BMF
BIK
Noxa

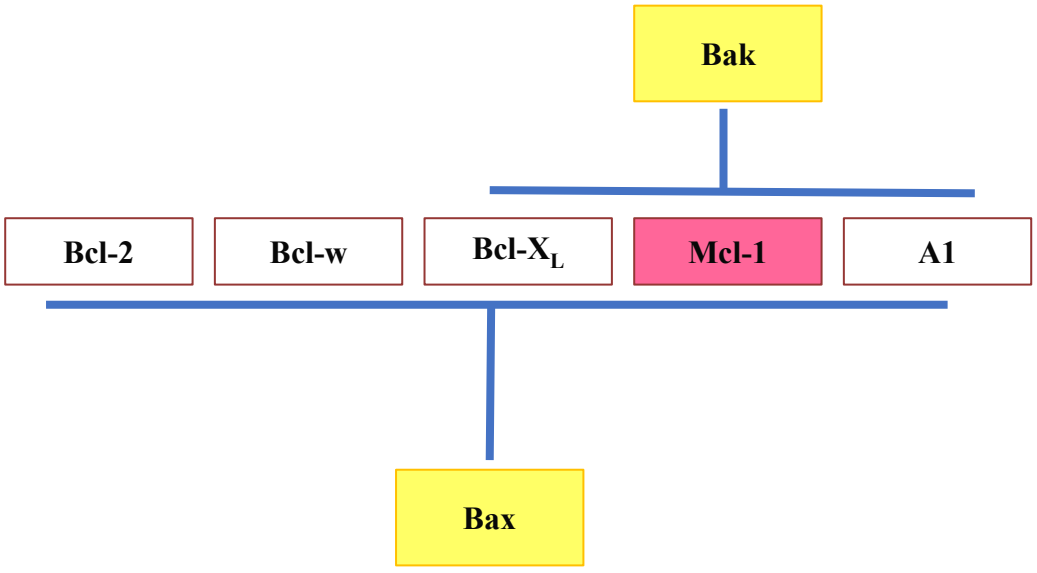
Bak
Bcl-2
Bcl-w
Bcl-X$_L$
Mcl-1
A1
Bax

1-5-1 The anti-apoptotic Bcl-2 family members in the nervous system

Knock-out and germline deletion models have shown that the Bcl-2 family members have unique and overlapping roles. Tissue specific knock-out of a gene of interest is possible via Cre/lox recombination. The gene of interest is flanked (floxed) by sequences known as loxP sites. These sites are recognized by the enzyme Cre recombinase, which is genetically inserted under a tissue-specific promoter, and Cre excises sequences between the loxP sites upon its translation. The tissue-specific promoter driving Cre expression results in the tissue-specific deletion of the protein of interest (Sauer, 1998).

Bcl-2 deficient mice survive to six months postnatal, but prematurely grey by six weeks and develop polycystic kidney disease (Veis et al., 1993). Bcl-2 is not required for the survival of the developing nervous system but has a postnatal role in the survival of motor neurons, sensory neurons and sympathetic neurons (Michaelidis et al., 1996). *Bcl-x* germline knock-out mice die by E14 due to erythroid progenitor cell death and neuronal cell death (Motoyama et al., 1995). When *bcl-x* is conditionally knocked-out in the nervous system using Nestin:Cre-mediated deletion, cell death begins at E11 and travels across the spinal cord following the progression of neuronal differentiation. Apoptosis peaks in the nervous system at E13 and mice are embryonic lethal by E18. Further analysis shows that cells of the spinal cord become dependent on Bcl-xL within 24 hours of initiating differentiation (Fogarty et al., 2016). Germline co-deletion of *bcl-x* and *bax* rescued most of the apoptosis that occurred in the nervous system of *bcl-x* null mice alone at E12 but did not rescue embryonic lethality and did not rescue the increased apoptosis seen in *bcl-x* null telencephalon-derived *in vitro* cultures (Shindler et al., 1997).

Nestin:Cre-mediated deletion of *bcl-x* and co-deletion of *bax* rescued apoptosis associated with *bcl-x* deletion alone in the nervous system (Fogarty et al., 2018). Bcl-xL has also been shown to be important in neurons of the upper layers of the cortex as well as the CA1-CA3 regions of the hippocampus (Nakamura et al., 2016). Deletion of *bcl-x* in these populations results in risk-taking behaviour, self injury and cognitive deficits in mice (Nakamura et al., 2016). Bcl-xL is also an important survival factor in rod photoreceptors, retinal ganglion cells and catecholaminergic neurons of the substantia nigra (Harder et al., 2012; Savitt et al., 2005; Zheng et al., 2006). Not all Bcl-2 family members have been implicated in nervous system development. For example, Bcl-w (Print et al., 1998) and A1 (Schenk et al., 2017) have not been found to play a significant role in the developing nervous system.

1-5-2 BH3-only proteins in the nervous system

Germline deletion of BH3-only proteins Bid, Bad or multi-domain pro-apoptotic Bak resulted in no change in cell death of superior cervical ganglion neurons upon trophic factor deprivation (Putcha et al., 2002). Germline deletion of Bim provided partial rescue of apoptosis in superior cervical ganglia and in the central nervous system upon trophic factor deprivation, implicating Bim as an important BH3-only protein in the nervous system (Putcha et al., 2001). Triple knock-out of Bim, Bid and PUMA resulted in similar defects in mice deficient in Bax and Bak such as imperforate vaginas and persistent interdigital webbing (Ren et al., 2010). Moreover, these mice were resistant to ionizing radiation exposure in adult cerebellar granule neurons (Ren et al., 2010).

Deletion of PUMA alone reduced apoptosis in irradiated cerebellar granulated neurons, but co-deletion of Bim and Bid was required to prevent apoptosis all together (Ren et al., 2010). Single deletion of Bad (Ranger et al., 2003) or Bid (Leonard et al., 2001) does not appear to have any neurological consequences.

1-5-3 Bax and Bak in the nervous system

The role of Bax and Bak in the nervous system has been studied; however, Bax has been studied more extensively than Bak. Bax expression has been detected in the primitive nervous system as early as E6, whereas expression of Bak does not occur in the nervous system until E12 (Krajewska et al., 2002). Bax deficient ($Bax^{-/-}$; BaxNull) male mice are sterile due to defects in sperm maturation, but otherwise survive (Knudson et al., 1995). BaxNull mice show increased neuronal numbers in superior cervical ganglia and the facial nuclei. In addition, sympathetic and facial motor neurons were resistant to apoptotic stimuli (Deckwerth et al., 1996). BaxNull mice also show increased cell numbers and reduced cell death in the dentate gyrus of the adult mouse hippocampus (Sun et al., 2004). Between E11.5 and postnatal day 1, deletion of Bax resulted in decreased cell death in spinal cord motor neuron pools, peripheral ganglia, the cerebellum, hippocampus, retina and trigeminal brainstem nuclear complex (White et al., 1998). *Bak* and *Bax* germline co-deletion ($Bax^{-/-}Bak^{-/-}$) is not embryonic lethal in mice, but many pups die shortly after birth and show classic signs of absent developmental apoptosis such as imperforate vaginas and webbed digits (Lindsten et al., 2000). $Bax^{-/-}$ $Bak^{-/-}$ showed circling behaviour and are unresponsive to auditory stimulation. Histology

revealed excessive numbers of small, chromatin dense cells in the regions surrounding the ventricles of the brain (Lindsten et al., 2000). $Bax^{-/-}Bak^{-/-}$ adult mice show excessive numbers of NPCs as well as immature neurons and glial cells in the brain demonstrating that effector proteins are responsible for reducing the population of NPCs in the brain. These cells were resistant to apoptotic stimuli; however, adult neurons were not resistant to death due to excitotoxicity (Lindsten et al., 2003). $Bak^{-/-}$ mice show no gross defects (Lindsten et al., 2000). These data demonstrate that Bax is the main pro-apoptotic effector member of the Bcl-2 family of proteins in the nervous system. Although Bax is important in regulating cell numbers in the developing brain, no research has elucidated how Bax activation is regulated in the developing nervous system.

1-6 Myeloid cell leukemia-1 (Mcl-1)

Mcl-1 is an anti-apoptotic member of the Bcl-2 family of proteins. It was originally discovered as a protein that was upregulated in response to myeloid cell differentiation in the ML-1 human myeloid leukemia cell line (Kozopas et al., 1993). Germline deletion of Mcl-1 is peri-implantation lethal at E3.5-E4 due to trophectoderm differentiation defects, making the study of Mcl-1 in other tissues challenging (Rinkenberger et al., 2000). The development of a floxed *mcl-1* mouse allowed insight into how Mcl-1 functions in different tissues via Cre/lox-mediated deletion. Conditional ablation of *mcl-1* in murine lymphocytes showed that both B and T lymphocytes are dependent on Mcl-1 for survival (Opferman et al., 2003). Conditional ablation of *mcl-1* in hematopoietic stem cells resulted in the destruction of bone marrow cell populations

(Opferman et al., 2005). Deletion of *mcl-1* in liver cells did not impact cell survival (Opferman et al., 2005).

Mcl-1 is unique among the anti-apoptotic proteins for many reasons. Firstly, Mcl-1 has only BH domains 1-3, unlike the other anti-apoptotic proteins, which have BH domains 1-4. Mcl-1 also has an elongated N-terminus. The N-terminus has many phosphorylation and ubiquitination sites. It also has many sequences known as PEST (proline, aspartic acid, serine and threonine) sequences. These PEST sequences make proteins more labile to degradation (Rechsteiner & Rogers, 1996). Overall, the PEST sequences, as well as the number of phosphorylation and ubiquitination sites found in the N-terminal region of Mcl-1 makes it highly modifiable with a short half-life compared to other Bcl-2 family members (Thomas et al., 2010; Yang et al., 1995).

1-7 Mcl-1 and neurogenesis

Conditional deletion of *mcl-1* in NPCs of the developing telencephalon with the use of either a FoxG1 or Nestin-mediated Cre (Mcl-1 CKO), revealed that Mcl-1 is an important anti-apoptotic factor in NPCs. Deletion of *mcl-1* results in massive apoptosis in the developing brain. This apoptosis extends throughout the course of neuronal differentiation in Nestin$^+$ NPCs, Doublecortin$^+$ migrating neuroblasts, and Tuj1$^+$ newly-born neurons in the developing forebrain. This massive apoptosis resulted in reduced cortical plate formation and embryonic lethality by E15.5-E16 in both deletion models. Further investigation using conditional deletion of *mcl-1* in cortical progenitors *in vitro* showed that the dependency on Mcl-1 is cell autonomous, whereas deletion of *mcl-1* in

cortical neurons did not result in increased cell death, but rather increased sensitivity to DNA damage (Arbour et al., 2008). *mcl-1* deletion in adult neurons, however, does not result in apoptosis without further death stimuli. Alternatively, it results in increased autophagy. Nutrient deprivation was shown to result in the endogenous degradation of Mcl-1, causing autophagy through de-repression of Beclin-1 (Germain et al., 2011). Mcl-1 has also been shown to be expressed in adult NPCs, and deletion of Mcl-1 in adult NPCs *in vitro* resulted in a doubling of apoptosis. Overexpression of Mcl-1 in adult NPCs *in vitro* reduced apoptosis (Malone et al., 2012). The results from these studies suggest that as NPCs differentiate, their dependency on Mcl-1 changes. NPCs, both embryonic and adult, depend on Mcl-1's anti-apoptotic properties, whereas adult neurons depend on Mcl-1 for its anti-autophagic properties. A third role for Mcl-1 in cell cycle exit of NPCs has been proposed. The potential for Mcl-1 to be involved in cell cycle dynamics has been discussed previously, but whether it impacted the cell cycle of neural cells was unknown. Overexpression studies have shown that Mcl-1 plays a role in the terminal mitosis of NPCs (Hasan et al., 2013).

Further investigation has shown that although the literature has suggested that Mcl-1 dependency and Bcl-xL dependency are sequential, NPCs are dependent on both Mcl-1 and Bcl-xL. Deletion of one allele of *bcl-x* in NPCs deficient in *mcl-1* will exacerbate the increase in cell death (Fogarty et al., 2018).

Although research has investigated the role of Mcl-1 in nervous system development, no research has determined if Mcl-1 is important for the survival of the nervous system when it initially forms during, and shortly after, neurulation. The pro-apoptotic effector protein that Mcl-1 inhibits in the developing nervous system is also

unknown. One candidate is Bax, which has been shown to be inhibited by Mcl-1, though this has not been shown in the nervous system (Germain *et al.*, 2008).

1-8 Hypothesis and Aims

The role of Mcl-1 in the early developing nervous system has not been fully characterized. Further, the relationship between anti-apoptotic Mcl-1 and pro-apoptotic effector activation has not been investigated, and therefore, the mechanism by which Mcl-1 inhibits apoptosis in the developing nervous system is yet to be elucidated.

I hypothesize that cells throughout the developing nervous system are dependent on Mcl-1 for survival, and this dependency is largely due to either the direct or indirect Mcl-1 inhibiting pro-apoptotic Bax (Figure 1-7). I will investigate my hypothesis using the following specific aims:

- Specific aim 1: Characterize the cell death in the developing nervous system of the Mcl-1 CKO.
- Specific aim 2: Determine the mechanism by which Mcl-1 inhibits apoptosis is the developing nervous system.

Figure 1-7. Hypothesis. **(A)** In the healthy condition and in the absence of apoptotic stimulation, Mcl-1 prevents apoptosis by inhibiting both BH3-only proteins and pro-apoptotic effector proteins. **(B)** The Nestin-mediated conditional deletion of Mcl-1 results in increased apoptosis in the developing nervous system as BH3-only proteins are no longer inhibited and can activate the pro-apoptotic effector protein Bax. **(C)** Co-deletion of Mcl-1 and Bax is hypothesized to rescue the apoptosis associated with the Mcl-1CKO alone as Mcl-1 inhibits apoptosis in the developing nervous system through the inhibition of pro-apoptotic Bax.

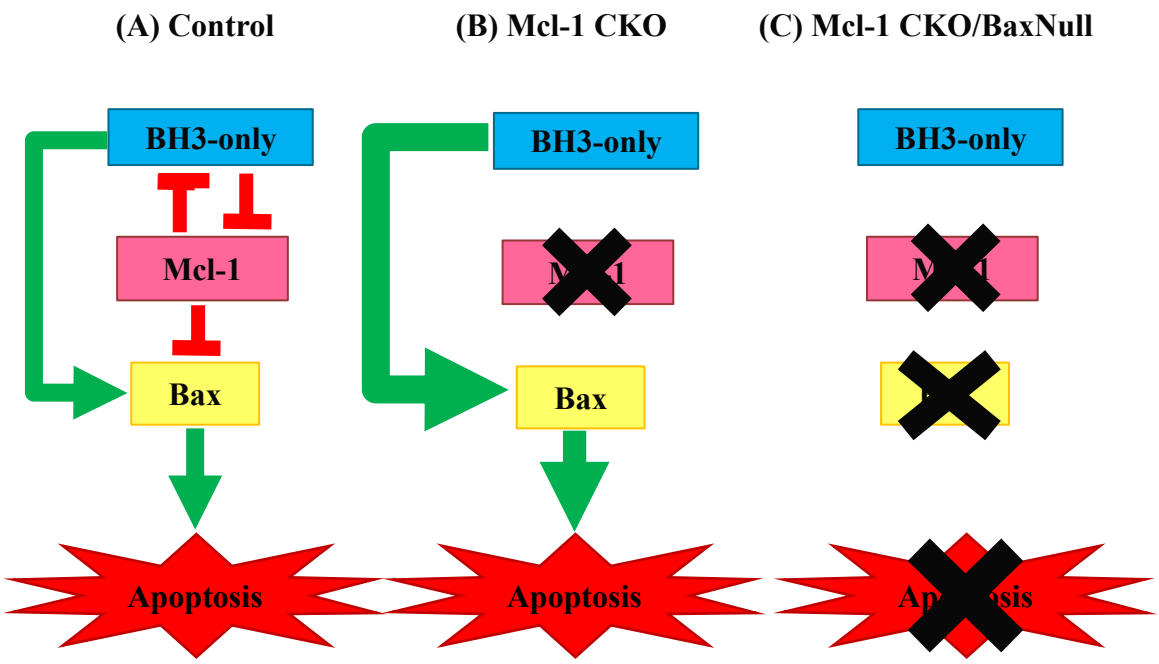
(A) Control
(B) Mcl-1 CKO
(C) Mcl-1 CKO/BaxNull
BH3-only
Mcl-1
Bax
Apoptosis
BH3-only
Bax
Apoptosis
BH3-only

2-0 Methods

2-1 Transgenic mouse line husbandry

Memorial University of Newfoundland's Animal Care Committee approved all experiments, which adhere to the Guidelines of the Canadian Council on Animal Care. Mice were housed on a 12-hour light/dark cycle and had access to food and water *ad libitum.* Transgenic mouse lines outlined in Table 2.1 below, were maintained on a C57Bl/6J background.

Table 2.1: Sources of transgenic mouse lines used in experiments.

Transgenic mouse line	Abbreviation	Provided by	Reference
mcl-1 floxed	(*mcl-1*$^{(f/f)}$)	In house	(Opferman et al., 2003)
bax Null	(*bax*$^{(-/-)}$)	002994 Jackson Laboratories, MN, USA	(Knudson et al., 1995)
bax floxed	(*bax*$^{f/f}$)	006329, Jackson Laboratories, MN, USA	(Takeuchi et al., 2005)
nestin mediated *cre*	(*nes:cre*$^{+/-}$)	In house	(Bérubé et al., 2005)

f= floxed, - = null, + = wild type

mcl-1$^{(f/f)}$ mice were crossed onto the *bax*$^{(-/-)}$ and *bax*$^{(f/f)}$ transgenic lines of mice to generate an *mcl-1*$^{(f/f)}$: *bax*$^{(-/f)}$ transgenic line. Due to sterility of both *mcl-1*$^{(f/f)}$ (Okamoto et al., 2014) and *bax*$^{(-/-)}$ (Knudson et al., 1995) males, only male mice with *mcl-1*$^{(+/f)}$:*bax*$^{(+/-)}$ or *mcl-1*$^{(+/f)}$:*bax*$^{(f/f)}$ were bred with female mice who could be one of many *mcl-1* or *bax* genetic combinations. For examples of genetic crosses and expected outcomes, see Appendix A.

2-2 Timed pregnancies

Male and female mice were placed in the same cage for a maximum of three days. Females were weighed at breeding. Twice daily, a metal probe was used to detect the presence of a white plug in the vagina of the female mouse. The presence of the plug was taken as embryonic day 0.5. Upon discovery of a plug, mice were separated, and the female was weighed between E9 and E11. Only mice that had a plug and steady weight-gain of at least three grams were assumed pregnant.

2-3 Tissue collection, cryo-protection

Mice were euthanized with an intraperitoneal injection of 300 µl of sodium pentobarbital (Euthanyl, 240 mg/ml, CDMV, QC, CA) followed by cervical dislocation. Post-euthanasia, embryos were removed. Embryos were collected at E9, E10 and E11. Sex of the embryos was not determined and both sexes were included and analyzed as a single group. For cryo-sectioning, brains and spinal cords were dissected under a Stemi 2000-C Stereo Microscope (Carl Zeiss Microscopy, LLC, USA). Embryos were then fixed in 4% v/v paraformaldehyde in phosphate buffered saline (1XPBS; 137 mM NaCl, 2.7 mM KCl, 10 mM Na_2HPO_4, 1.8 mM KH_2PO_4), pH 7.4 overnight at 4°C. The following day, embryos were cryoprotected in a 30% w/v sucrose solution in 1XPBS until the embryo sank (approximately 24 hours). Next, tissue was further dissected into forebrain, brainstem, and three spinal cord sections, wicked free of residual moisture and placed in Tissue-Tek® O.C.T. compound embedding medium (Sakura Finetek, 4583, CA, USA). Embedded tissue was frozen in isopentane cooled by dry ice. Tissue was stored long-term at -80°C.

2-4 Cryo-sectioning of tissue

Embedded tissue was sectioned into 14µm thick sections using a Micron HM 520 Cryostat (8243-30-1015, GMI, MN, USA). Sections were collected onto *Superfrost Plus* Microscope Slides (12-550-15, Fisher Scientific, PA, USA). Serial sections were collected across 6 slides each and after the sixth slide, four sections were discarded. Thus, sections on a given slide represented anatomical regions 140 µm (10 sections) apart. One slide per set was saved for staining using cresyl violet for general histology and landmarking purpose (section 2-7 Cresyl violet staining). After sectioning, slides were stored at -80ºC.

2-5 Genotyping

Adult transgenic mice were genotyped to identify the transgenic make-up of a given mouse. Prior to weaning, all mice received an ear-tag that gave each mouse a numerical identity. A small piece of the tail tip was collected for genotyping. All transgenic embryos were genotyped post-dissection. While dissecting transgenic embryos, forelimbs were removed and divided into two microcentrifuge tubes for genotyping. One sample was frozen at -20ºC as a back up sample and one was used for genotyping. After tissue collection, processing of tissue and genotyping was identical for both embryonic and adult tissue. DNA extraction was carried out using a modified protocol of the REDExtract-N-Amp™ Tissue PCR Kit (XNAT-100RXN, Sigma-Aldrich Co. LLC, MO, USA). Tissue was digested overnight at 55ºC on a heat block in 70 µl of "Extraction Buffer" and 12 µl of "Tissue Prep". The following day, samples were

vortexed vigorously and heated to 95ºC for 3 minutes before the addition of 70 µl "Neutralization Buffer".

Genotyping for *mcl-1*, *bax*, and *cre* was carried out via Polymerase Chain Reaction (PCR) using One*Taq* DNA Polymerase (M0480L, New England Biolabs, Inc., MA, USA). Primers and product sizes used for PCR are outlined in Table 2.2, reaction buffer recipes for each gene are outlined in Table 2.3, and the DNA Engine Peltier Thermal Cycler (ALD1244, BioRad, CA, USA) parameters are outlined in Table 2.4, below. Post-amplification, samples were loaded with DNA loading buffer (30% Glycerol, 1 mM EDTA; pH 8.0, 0.06% bromophenol blue (BPB)) and run on a 2% UltraPure™ Agarose gel (16500-500, Invitrogen, CA, USA) in TAE (40 mM Tris-acetate, 1 mM EDTA) with ethidium bromide (15585011, Invitrogen, CA, USA) at 120 V using a BioRad PowerPac™ Basic Power Supply (1645050, BioRad, CA, USA) until positive control bands were resolved, which were visualized using an ultraviolet transilluminator.

Table 2.2: Genotyping primer sets and product sizes.

Gene	Primer set	Expected product sizes
mcl-1 floxed	6 Mcl-1 5'-GCAGTACAGGTTCAAGCCGATG-3' 7 Mcl-1 5'-CTGAGAGTTGTACCGGACAA-3'	Wildtype:360bp Floxed: 400bp
bax floxed	Baxf FOR 5'-GAATGCCAAAAGCAAACAGACC-3' Baxf REV 5'-ACTAGGCCCGGTCCAAGAAC-3'	Wildtype:244bp Floxed: 340bp
bax Null	Bax1 5'-TGATCAGAACCATCATG-3' Bax2 5'-GTTGACCAGAGTGGCGTAGG-3' Bax3.1 5'-CCGCTTCCATTGCTCAGCGG-3'	Wildtype:304bp Null: 507bp
cre	CRE-3B 5'-TGACCAGAGTCATCCTTAGCG-3' CRE-5B 5'AATGCTTCTGTCCGTTTGCC-3'	Presence:700bp No *cre*: no product

Table 2.3: PCR reaction buffer components for genotyping.

	Volume per reaction (µl)							
	***mcl-1* floxed**		***bax* floxed**		***bax* Null**		***cre***	
5X OneTaq Reaction Buffer		10		10		10		10
Primers (2.5 µM)	6 Mcl-1	5	FOR	5	Bax1	10	3B	4
	7-Mcl-1	5	REV	5	Bax2	5	5B	4
					Bax3.1	5		
dNTPs (1.25 mM)		8		8		8		8
H_2O		17.75		17.75		7.75		21.75
One*Taq* DNA Polymerase		0.25		0.25		0.25		0.25
DNA		4		2		4		2

Table 2.4: Thermal cycler parameter for genotyping PCRs.

Step	***mcl-1* floxed**			***bax* floxed**		
1	94ºC	5.0 min		94ºC	3.0 min	
2	94ºC	1.0 min	Steps 2-4	94ºC	30 sec	Steps 2-4
3	56ºC	1.0 min	X 30	68ºC	1.0 min	X 35
4	72ºC	1.0 min		72ºC	1.0 min	
5	72ºC	1.0 min		72ºC	2.0 min	
6	10ºC	Hold		10ºC	Hold	
	***bax* Null**			***cre***		
1	94ºC	5.0 min		94ºC	2.0 min	
2	94ºC	1.0 min	Steps 2-4	94ºC	1.0 min	Steps 2-4
3	55ºC	1.0 min	X 30	56ºC	1.0 min	X 30
4	72ºC	1.0 min		72ºC	1.5 min	
5	72ºC	3.0 min		72ºC	5.0 min	
6	10ºC	Hold		10ºC	Hold	

2-6 Immunofluorescence

All washes were at room temperature with shaking on a benchtop rotator unless stated otherwise. Slides were taken directly from -80ºC and placed on 37ºC slide warmer

for 20 minutes. While warming, a Dako Pen (S2002, Dako Denmark, Denmark) was used to draw a hydrophobic barrier around sections of the slide. Slides were then washed in 1XPBS twice for 5 minutes. After, slides were placed in a humidity chamber. Active Caspase 3 (AC3) rabbit IgG monoclonal primary antibody solution in 1XPBS ([1:400], 559565, BD-Pharmingen, CA, USA) was then applied to the slide. The container was sealed overnight at room temperature without shaking. The following day, slides were washed three times in 1XPBS, placed in a humidity chamber and incubated with secondary donkey anti-rabbit IgG (H+L) AlexaFluor 488 nm antibody solution ([1:200], A21206, Invitrogen, CA, USA) for one hour at room temperature in the dark. Following secondary antibody application, all remaining procedures were carried out in opaque containers to prevent photo-bleaching of the secondary antibody fluorochromes. Slides were washed three times in 1XPBS and then stained in 40 µg/ml Bisbenzimide H33258 to stain nuclei (Hoechst 33258; B1155, Sigma-Aldrich Inc, MO, USA) in 1XPBS for 2 minutes at room temperature. Slides were then washed twice in 1XPBS and coverslipped with 3:1 1XPBS:Glycerol as a mounting media and Fisherbrand Microscope Cover Glass (12545C, Fisher Scientific, NH, USA). Edges of the coverslips were sealed using nail polish. Slides were stored at -20ºC.

2-7 Cresyl violet staining

One slide (5A, 10A, etc.) from each set of sectioned tissue was stained using cresyl violet for histology. Unless otherwise stated, all incubations occurred at room temperature without shaking in a fume hood. Slides were heated at 37ºC for 20 minutes followed by incubation in 0.1% w/v cresyl violet in water for 8-12 minutes. Post-

incubation, slides were washed for 5 minutes in water to remove excess stain. Tissue was then dehydrated by submerging in increasing concentrations of ethanol for 30 seconds at each concentration (50%, 75%, 90%, 95%, and 3 times in 100% v/v ethanol in water). Next, slides were placed in isopropanol for 30 seconds, followed by two washes in toluene for 1 minute each. Slides were coverslipped using Permount® (SP15-500, Fisher Chemical, NJ, USA) and Fisherbrand Microscope Cover Glass (12545C, Fisher Scientific, NH, USA). After coverslipping, slides were left in the fume hood overnight to dry.

2-8 *In vitro* neurosphere cell culturing

Timed pregnant females were euthanized by a lethal injection of sodium pentobarbitol (Euthanyl, 240 mg/ml, CDMV, QC, CA) followed by cervical dislocation. Embryo forebrains were removed and dissected in ice-cold Hanks' Balanced Salt Solution (14065-056, Gibco, NY, USA; pH 7.4). The ganglionic eminence was isolated and triturated gently in 37ºC stem cell media (see table 2.5) 30-40 times, until dissociated. Cells were then counted with a hemocytometer using 0.4% Trypan Blue (15250-061, Gibco, NY, USA). $3.3x10^5$ cells were plated in 3 ml of 37ºC stem cell media. Cells were cultured at 37ºC with 5% CO_2 for 3 days in a Forma Series II Water Jacket CO_2 Incubator (Thermo Fisher Scientific, 3110, OH, USA). After 3 days, neurospheres were used for experiments or differentiated. To differentiate neurospheres, 20-30 neurospheres between 100-150 µm in diameter were individually plucked using a pipette and placed in Lab-Tek 8 well Chamber Slides (177402, Thermo Scientific Nunc, NY, USA) containing 400 µl Differentiation Media (Table 2.6). Slides were pre-coated

with 0.0015% Poly-L-ornithine (P4957, Sigma Life Sciences, MO, USA) in sterile, distilled water for 1 hour at room temperature. Cells were incubated in the same conditions as the neurospheres (37ºC, 5% CO_2) for 1, 3 or 7 days.

Table 2.5: Stem cell media components for *in vitro* culturing.

Reagent	Concentration	Source
Dulbecco's Modified Eagle Medium Nutrient Mixture F-12 (Ham) (DMEM/F12) (1:1) [+] L-Glutamine [+] 15 mM HEPES	Base	11330-032, Gibco, NY, USA
D-(+)-Glucose	5.85 mg/ml	G7528-250G, Sigma, MO, USA
l-glutamine	1.95 mM	25030081, Invitrogen, CA, USA
Pen Strep (Penicillin Streptomycin)	48.7 units/ml	15140, Gibco, NY, USA
Insulin	24.4 µg/ml	I-5500-250MG, Sigma, MO, USA
Apotransferrin	97.4 µg/ml	11096-37-0, Sigma, MO, USA
Progesterone	0.0194 nM	P8783-1G, Fisher, NY, USA
Putrescine	9.36 µg/ml	P5780-5G, Sigma, MO, USA
Selenium	2.92 nM	S5261-10G, Sigma, MO, USA
Fungizone	12.1 ng/ml	15290018, Invitrogen, CA, USA
Heparin	1.95 µg/ml	H3149-50KU, Sigma, MO, USA
bFGF	0.195 µg/ml	F0291-25UG, Sigma, MO, USA

Table 2.6: Differentiation media components for *in vitro* culturing.

Reagent	Concentration	Source
Neurobasal® Media [-] L-Glutamine	Base	21103-049, Gibco, NY, USA
Fetal Bovine Serum	1%	F2442, Sigma, MO, USA
L-glutamine	0.5 mM	25030081, Invitrogen, CA, USA
N2 Supplement	1%	17502-048, Invitrogen, CA, USA
B27 Supplement	2%	17502-044, Invitrogen, CA, USA
Pen Strep	50 units/ml	15140, Gibco, NY, USA
Fungizone	12.1 ng/ml	15290018, Invitrogen, CA, USA

2-9 Immunocytochemistry

Cell cultures were fixed with -20 ºC 1:1 acetone:methanol for 5 minutes, followed by washes in cold 1XPBS. AC3 Rabbit IgG monoclonal primary antibody solution in 1XPBS ([1:400], 559565, BD-Pharmingen, CA, USA) was incubated with cells overnight at 4 ºC. The following day, cells were washed 3 times with 1XPBS and next, they were incubated with secondary Donkey anti-rabbit IgG (H+L) AlexaFluor 488nm antibody solution ([1:200], A21206, Invitrogen, CA, USA) in the dark. After incubation, cells were washed twice with 1XPBS followed by incubation in 40 µg/ml Bisbenzimide H33258 to label nuclei for two minutes. After two final washes, chambers from chamber slides were removed and slides were coverslipped and sealed with nail polish.

2-10 Microscopy

All immunostained tissue and cell cultures were imaged using a Zeiss AxioImager Z.1 microscope (Carl Zeiss Microscopy, Jenna, Germany). A Colibri LED light source

was the source of the fluorescence (Carl Zeiss Microscopy, Jenna, Germany). Images were acquired in 12-bit greyscale using a Zeiss AxioCam MRm camera (Carl Zeiss Microscopy, Jenna, Germany) and processing, including false colouring and image overlaying, was completed using Zeiss AxioVision v4.8 software (Carl Zeiss Microscopy, Jenna, Germany). Figures were compiled with Adobe Photoshop CS5 Extended 12.0.4 X64 (Adobe Inc, CA, USA) and Microsoft PowerPoint 2016 (Microsoft Inc, WA, USA). Contrast and brightness adjustments were applied equally across all images.

2-11 Cell counts

Cell counts were manually completed using FIJI (Fiji Is Just ImageJ; https://fiji.sc/) software (Schindelin et al., 2012). For AC3 counts in forebrain sections, a 125 µm x 125 µm region of interest (ROI) was placed over the medial portion of the medial ganglionic eminence, anterior to the caudal ganglionic eminence and inferior to the lateral ganglionic eminence. For AC3 counts of the spinal cord, a 125 µm x 125 µm ROI was placed in the dorso-medial cervical spinal cord, which was identified as at the level of the cervical enlargement. Cells were defined as apoptotic if they were immunopositive for AC3 and had a condensed nucleus, as visualized with Hoechst stain. Apoptotic cells were counted out of the total number of Hoechst positive nuclei. For both brain and spinal cord counts, three representative regions were counted per embryo. For immunocytochemistry, a field of view at 20X was used as the region to count. For each culture, four representative regions were counted.

2-12 Western blotting

2-12-1 Protein extraction

Tissue samples were dissected as described above. Samples were kept on ice. 200 µl of complete immunoprecipitation buffer (complete IP buffer; 25 mM Tris, pH 7.4, 150 mM NaCl, 1 mM CaCl, 1% Triton X-100 (93426, Sigma, MO, USA), 200 µg/ml phenylmethylsulfonyl fluoride (P7626, Sigma, MO, USA), 1µg/ml aprotinin (A-6103, Sigma, MO, USA) 1 µg/ml leupeptin (L-2882, Sigma, MO, USA), 1mM dithiothreitol (DTT; 43816, Sigma, MO, USA)) was added to each sample. Samples were triturated to break up the tissue and incubated on ice for 3 minutes. Samples were triturated until milky, which is indicative of complete tissue breakdown, and incubated on ice for 10 more minutes. Trituration was repeated until samples were completely homogenous. Samples were then centrifuged at 2000 rotations per minute (rpm) at 4℃ for 5 minutes using an Eppendorf Centrifuge 4417R (Hamburg, Germany) and supernatants were transferred to new prechilled microcentrifuge tubes.

2-12-2 Protein concentration determination

BioRad Protein Determination Assay reagent (500-0006, BioRad, CA, USA) was used to determine the concentration of extracted protein. 5 µl of a 1:5, 1:10 and 1:15 dilution of protein sample in complete IP buffer was added to 795 µl of ddH_2O. 200 µl of the BioRad Protein Determination Assay reagent was added to each sample and samples were incubated at room temperature before reading absorbance with a Thermo Scientific Genesys 10 UV Scanning spectrophotometer (WI, USA) at 595 nm. Sample absorbances were compared to a standard curve of Bovine Serum Albumin (BSA; Standard curve

from 0-7.5 ug/ml; B4287, Sigma, MO, USA) to interpolate sample protein concentration using the following formula:

$$Sample\ concentration\ [\mu g/\mu l] = \left[\frac{(average\ sample\ absorbance)}{Volume\ of\ Sample(\mu l) * slope}\right] * Dilution\ Factor$$

2-12-3 Sample electrophoresis and western blotting

Prior to western blotting, protein samples were separated via sodium dodecyl sulfate polyacrylamide gel electrophoresis (SDS-PAGE). For each sample, 35 µg of protein was used. The volume of each sample was brought to 20 µl by adding complete IP buffer. 5 µl of 5X loading buffer (250 mM Tris-HCl (pH 6.8), 0.5 M DTT, 10% Sodium Dodecyl Sulfate (SDS; 15525-017, Invitrogen, CA, USA), 0.5% Bromophenol Blue (BPB; B392-5, Fisher Scientific, NJ, USA), 50% Glycerol) was added to each sample, and samples were mixed and boiled in a water bath for 5 minutes. Entire sample volumes were loaded into a 10% polyacrylamide gel (see Table 2.7 below for gel recipe) and were run in a Bio-Rad Mini-PROTEAN® Tetra Cell (1658003, CA, USA) a BioRad PowerPac™ Basic Power Supply (1645050, BioRad, CA, USA) at 80 V in running buffer (50 mM Tris, 150 mM glycine, 3.5 mM SDS). After samples had passed through the stacking gel, the power was increased to 110 V for 2.5 hours. 5 µl of Bio-Rad Precision Plus Protein ™ Standards Kaleidoscope™ (#161-0375 Rev B, CA, USA) was run as a molecular weight ladder. Protein samples were then transferred from the gel to a 0.2 µm nitrocellulose membrane (1620112, Bio-Rad, CA, USA) using a Bio-Rad Mini Trans-

Blot ® Cell (1703930, BioRad, CA, USA) at 290 mA for 90 minutes in cold transfer buffer (25 mM Tris, 150 mM glycine, 20% v/v methanol).

Table 2.7: SDS PAGE gel recipes

	10% Separating Gel	**4% Stacking Gel**
ddH_2O	7.0 ml	4.05 ml
0.5 M Tris, 1.5 M glycine (pH 8.8)	4.0 ml	/
0.5 M Tris-HCl (pH 6.8)	/	1.4 ml
10% SDS	0.8 ml	0.4 ml
50% glycerol	2.0 ml	1.0 ml
40% arcylamide, 0.25% bisacrylamide	5.0 ml (filtered)	1.25 ml (filtered)
Ammonium persulphate	30 mg in 1 ml ddH_2O	25 mg in 1 ml ddH_2O
TEMED	0.02 ml	0.01 ml
Total volume	20ml	10ml

Post-transfer, the membrane was washed in Tween-20 Phosphate Buffered Saline (TPBS; 5 mM NaH_2PO_4, 20 mM Na_2HPO_4, 154 mM NaCl, 0.1% Tween 20) at room temperature 2X 10 minutes. Next, the blot was blocked in 5% blotto (5% skim milk powder in TPBS) for 1 hour followed by two washes in 0.5% blotto for 5 minutes each. Blot was incubated overnight at 4℃ in primary anti-Mcl-1 antibody ([1:1000]; 600-401-394, Rockland, PA, USA) in 0.5% blotto. The following day, blots were washed twice in 0.5% Blotto for 10 minutes each and the appropriate Horse Radish Peroxidase (HRP)-conjugated secondary antibody (Goat anti-Rabbit IgG HRP conjugate; 1706515, BioRad, CA, USA) at [1:2000] in 0.5% Blotto was incubated with the blot for one hour at room temperature. Blots were washed in TPBS twice for 10 minutes each and then developed with the Western Lightning Plus-ECL Enhanced Chemiluminescence Kit (02118 2512, Perkin Elmer Labs Inc., MA, USA) according to manufacturers instructions. Blots were

imaged using a GE ImageQuant LAS 4000 (28 9558 10, GE Healthcare, QC, CA). Post-imaging, blots were stripped of antibodies using Western Blot Stripping Buffer (21059, Sigma, ON, CA) at 37℃ for 20 minutes, then washed three times in TPBS for 5 minutes, followed by 5 minutes in 0.5% blotto. Blots were blocked as described, above. Next, blots were incubated with anti-β-Actin ([1:5000], A5316, Sigma, ON, CA) in 0.5% blotto overnight at 4℃. Blots were washed in 0.5% blotto, incubated in secondary antibody (Goat anti-mouse IgG HRP conjugate, 1706516, BioRad, CA, USA), washed in TPBS and imaged as described above. β-Actin was used as an internal control for the quantity of protein loaded.

2-12-4 Western Analysis

Western blot band densitometry was performed using FIJI software (Schindelin et al., 2012). Background was subtracted with a rolling ball radius of 50px. Band density was calculated in arbitrary units (A.U.) and was normalized to β-actin or GAPDH by dividing the A.U. of Mcl-1 to the A.U. of β-actin to control for the quantity of protein loaded. Normalized values were compared between samples. For Mcl-1, band density was calculated as the total density of the doublet of bands observed. For each experiment, three blots were analyzed.

2-13 Statistical analysis

All statistical analyses were completed using GraphPad Prism 5.02 (GraphPad Software, Inc, CA, USA). Tissue cell counts were analyzed with a parametric one-way

ANOVA with post-hoc analysis using Tukey's multiple comparison test. *In vitro* cell counts were analyzed with a parametric two-way ANOVA with Bonferroni post-hoc test. Western blots comparing control to knockout tissue were analyzed with two-tailed paired t-tests, where each control sample was paired with a corresponding knock-out sample run in the adjacent lane. For all experiments, a p-value less than 0.05 was considered significant.

3-0 Results

3-1 Onset of Mcl-1 expression during neurogenesis.

Expression of Mcl-1 has been shown in the developing nervous system, but only at E10, E11.5, and E15.5 (Arbour et al., 2008; Fogarty et al., 2018). These studies demonstrated that Mcl-1 was expressed throughout the nervous system in both precursor and differentiated populations. Investigation into Mcl-1 expression has shown Mcl-1 is expressed in early embryonic tissue up to E6 (Rinkenberger et al., 2000). No study has investigated if Mcl-1 is expressed in the early nervous system prior to E10 during neurulation. To investigate if Mcl-1 is expressed during early neurulation at E8, a western blot for Mcl-1 tissue was performed (Figure 3-1). Although RNA *in situ* hybridization or immunohistochemistry for Mcl-1 would be an appropriate technique, challenges in developing protocols that result in a clear Mcl-1 signal have precluded these analyses. Heads of E8 wild-type C57Bl/6J embryos were collected and Western analysis was performed. E10 and E12 forebrain tissue samples were run as a point of comparison. Western blotting for Mcl-1 often results in multiple bands. This has been attributed to post-translational proteolytic cleavage of Mcl-1 (Perciavalle et al., 2012; De Biasio et al., 2007; Huang & Yang-Yen, 2010). Due to challenges dissecting tissue, contamination by non-neural tissue was unavoidable. Nonetheless, expression of Mcl-1 was seen in E8 heads, showing that Mcl-1 is expressed at E8 (n=2 blots).

Figure 3-1. Mcl-1 protein expression is observed at E8. **(A)** Western blots for Mcl-1 in C57BL/6J wild-type E8 embryonic heads compared to E10 and E12 forebrain expression. Each E8 head sample contained one pooled litter. Each E10 sample contained 3 pooled nervous system samples and each E12 sample contained 2 pooled nervous system samples. **(B)** Densitometry analysis of Mcl-1 protein levels. Mcl-1 protein levels (A.U.) were normalized to GAPDH.

A

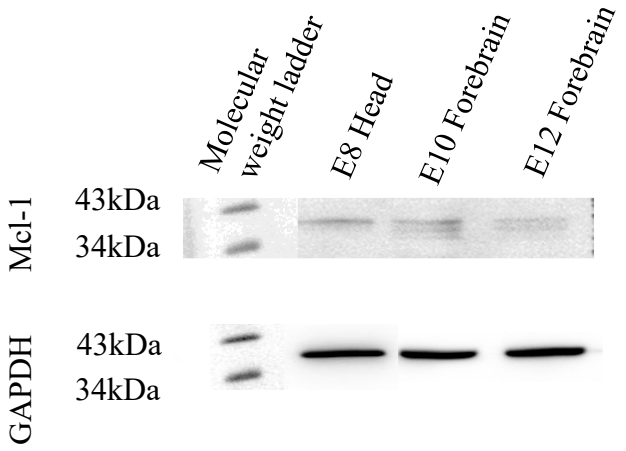
Molecular weight ladder
E8 Head
E10 Forebrain
E12 Forebrain
Mcl-1
43kDa
34kDa
GAPDH
43kDa
34kDa

B

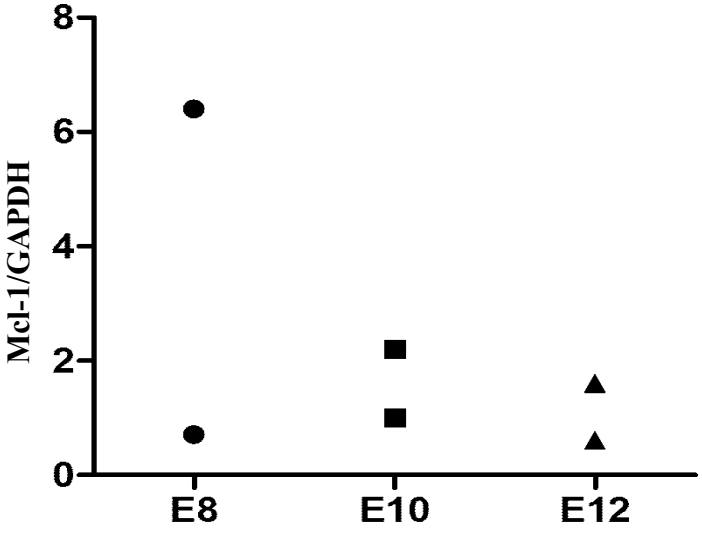
Mcl-1/GAPDH
8
6
4
2
0
E8
E10
E12

3-2 Mcl-1 protein in the Mcl-1 CKO.

Complete deletion of *mcl-1* has been shown in forebrains, brainstems and spinal cords in E12 Mcl-1 CKO tissue (Fogarty et al., 2016). The effectiveness of the deletion of *mcl-1* has not been investigated at prior timepoints. To study the effect of *mcl-1* deletion during early nervous system development, the effectiveness of the deletion of *mcl-1* needed to be investigated. Protein levels of Mcl-1 in the nervous system of E10 wild-type embryos were compared to the nervous system of Mcl-1 CKOs to determine if Mcl-1 was effectively excised at the onset of apoptosis. E10 forebrains, brainstems and hindbrains were analyzed, separately. (Figure 3-2A; n=3 for each group). Densitometry revealed that of the forebrain, brainstem and spinal cord, only the forebrain showed a significant decrease in Mcl-1 protein levels [paired t-test $t(2)=8.943$, $p<0.05$]. The brainstem and spinal cord, however, showed a non-significant decrease (Figure 3-2B; $p=0.0733$ for brainstem and $p=0.222$ for the spinal cord). None of the knock-out tissue showed a complete excision of *mcl-1*. Challenges in separating the small, delicate E10 nervous system from the other developing tissue may have resulted in tissue contamination. The tissue of embryos at E10 was softer and the nervous system much smaller than at E12 causing challenges in separating neural from non-neural tissue.

Figure 3-2. Mcl-1 protein expression in CTLs compared to Mcl-1 CKOs at E10. **(A)** Western blot analysis of E10 forebrain, brainstem and spinal cord tissue for Mcl-1 protein shows that Mcl-1 was reduced but not absent in Mcl-1 CKOs. Each lane represents three pooled embryos. β-Actin was used as a control for amount of protein loaded. **(B, C, D)** Densitometry analysis of Mcl-1 doublet to assess protein levels. Mcl-1 protein levels were normalized to β-Actin. Control and Mcl-1 CKO protein levels were compared separately in E10 **(B)** forebrain, **(C)** brainstem and **(D)** spinal cords using a two-tailed paired t-test. Three blots were analyzed for each group. *$p<0.05$, Error bars represent +/- Standard Deviation (SD).

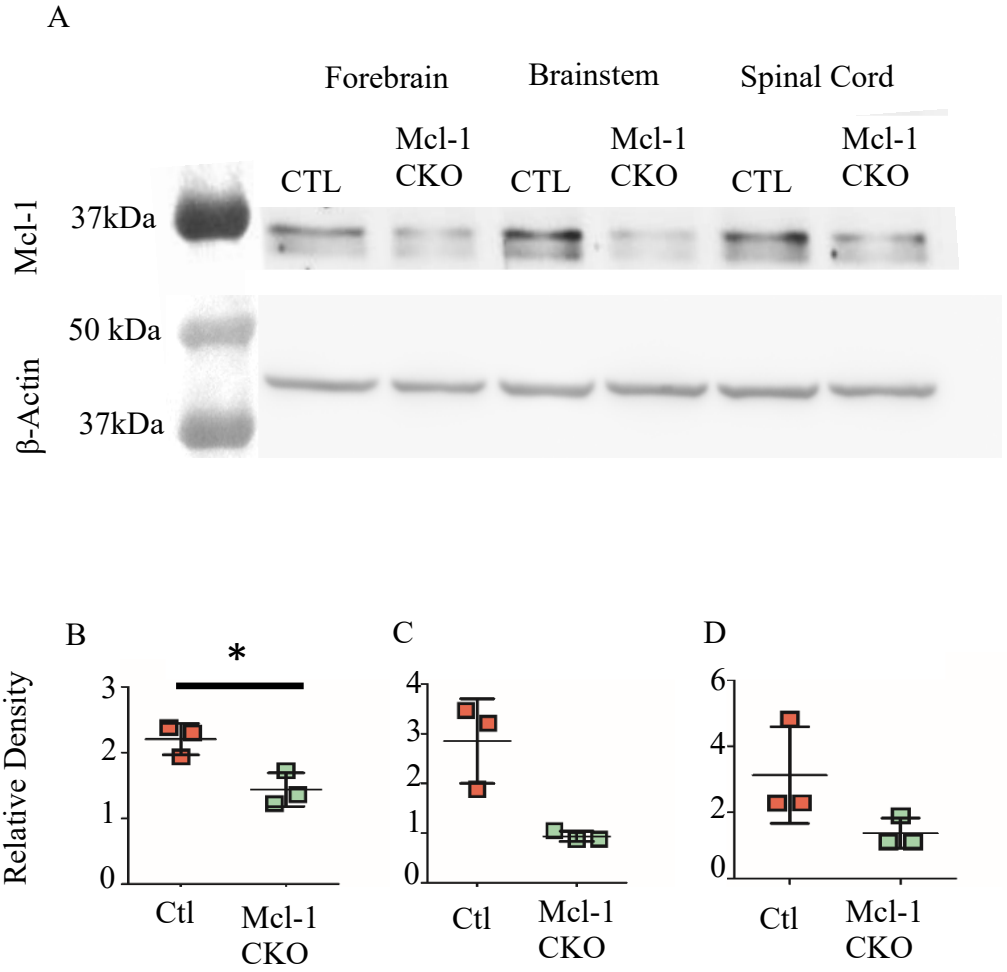
A
Forebrain
Brainstem
Spinal Cord
CTL
Mcl-1 CKO
CTL
Mcl-1 CKO
CTL
Mcl-1 CKO
Mcl-1
37kDa
50 kDa
β-Actin
37kDa
B
C
D
Relative Density
*
3
2
1
0
4
3
2
1
0
6
4
2
0
Ctl
Mcl-1 CKO
Ctl
Mcl-1 CKO
Ctl
Mcl-1 CKO

3-3 Onset of apoptosis in Mcl-1 CKO forebrains.

The apoptosis that occurs in the forebrain of the Mcl-1 CKO has been characterized previously at E12.5 (Arbour et al., 2008); however, the timing of the onset of apoptosis has not been identified. In order to investigate the onset of apoptosis in the early developing brain of the Mcl-1 CKO, immunofluorescence for AC3 was performed on forebrains from E9, E10 and E11 CTL and Mcl-1 CKOs. AC3 immunofluorescence showed that endogenous rates of apoptosis were low in control tissue at E9 (n=3), E10 (n=2) and E11 (n=4) (Figure 3-3B). High magnification revealed full nuclei, as shown by Hoechst staining (Figure 3-3B'). Low magnification of Mcl-1 CKOs revealed no apoptosis at E9 (n=3), but by E10 (n=2), apoptosis had begun in the developing ganglionic eminences of the forebrain. Apoptosis continued in the E11 (n=4) lateral and medial ganglionic eminences (Figure 3-3C). Higher magnification of the Mcl-1 CKO revealed that at E9, as seen in the lower magnification, no apoptosis was observed, as no AC3 staining was present and nuclei were not condensed. The onset of apoptosis was observed at E10, with AC3 co-localizing with condensed nuclei, as visualized with Hoechst staining. This apoptosis continued at E11 (Figure 3-3C'). This demonstrates that in the Mcl-1 CKO, apoptosis begins in the forebrain at E10.

Figure 3-3. Apoptosis in the forebrain of E9-E11 Mcl-1 CKOs. (**A)** Diagram of E9-E11 embryos demonstrating the location in the forebrain where AC3 immunofluorescence was performed. **(B)** Representative images of active Caspase-3 (AC3) immunostained (grey) CTL sections from E9, E10 and E11 embryos. **(B')** 20X magnification of CTL showing Hoechst stained nuclei (grey) and AC3 immunostaining (green). **(C)** Representative images of AC3 immunostained (grey) Mcl-1 CKO sections from E9, E10 and E11 embryos **(C')** High magnification of Mcl-1 CKO sections showing Hoechst stained nuclei (grey) and AC3 immunostaining (green).

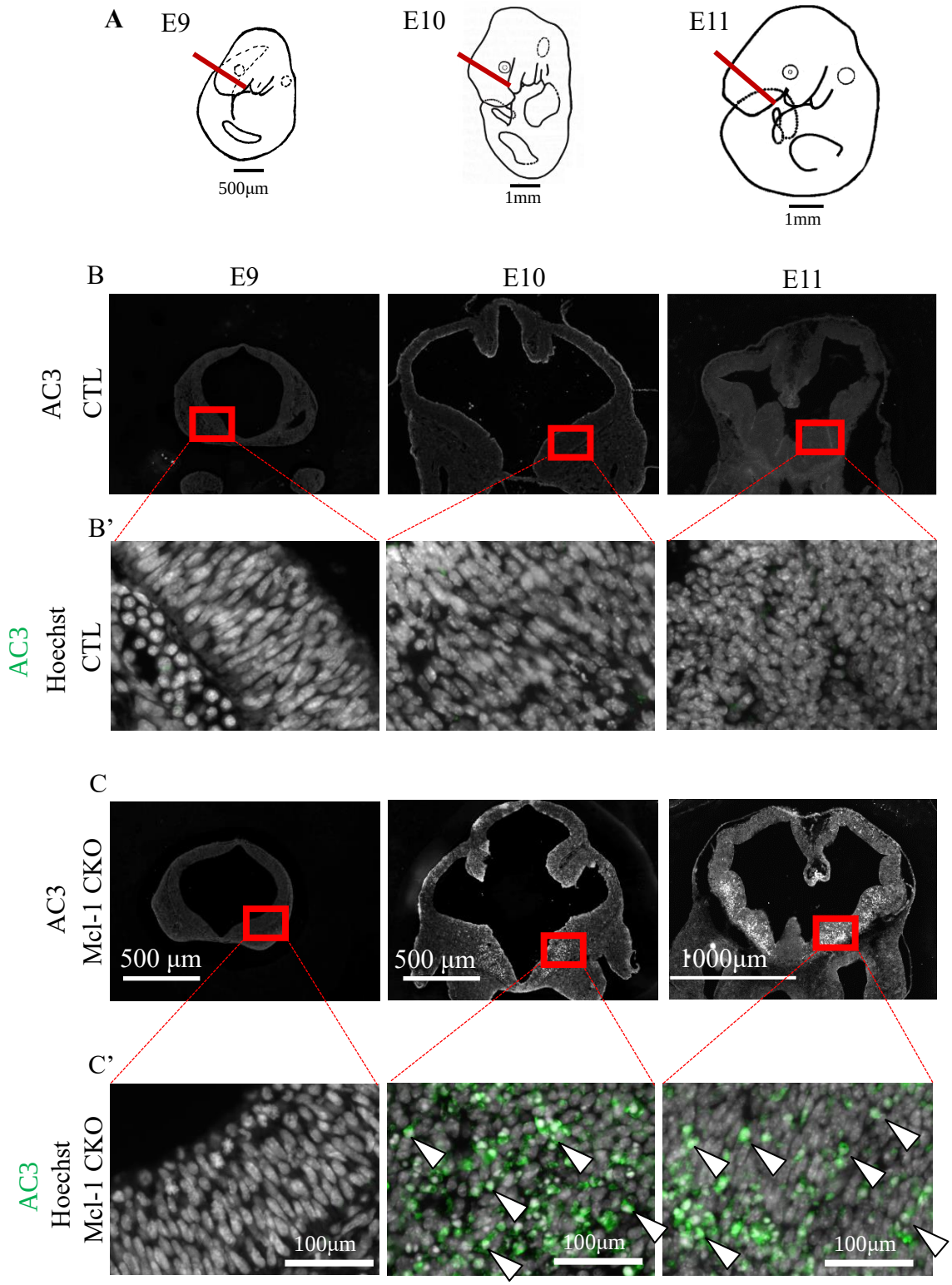
A
E9
E10
E11
500µm
1mm
1mm
B
E9
E10
E11
AC3
CTL
B'
AC3
Hoechst
CTL
C
AC3
Mcl-1 CKO
500 µm
500 µm
1000µm
C'
AC3
Hoechst
Mcl-1 CKO
100µm
100µm
100µm

3-4 Progression of apoptosis in Mcl-1 CKOs brainstem and spinal cord.

The progression of apoptosis in the Mcl-1 CKO has not been previously characterized in the developing brainstem and spinal cord. To address the role of Mcl-1 in the developing brain and spinal cord, AC3 immunofluorescence was used as a marker for apoptosis in combination with condensed nuclear staining. It was shown that endogenous rates of apoptosis were low in littermate control E9 (n=3), E10 (n=2) and E11 (n=4) brainstems, upper spinal cords and lower spinal cords (Figure 3-4A). In stark contrast, Mcl-1 CKOs showed AC3 immunopositivity beginning at E9 (n=3) in the ventral brainstem and rostro-ventral spinal cord, with no AC3 immunopositivity in the caudal spinal cord. By E10 (n=2), apoptosis had spread across to encompass the entire brainstem, while both the rostral and caudal spinal cords had apoptosis ventrally. At E11 (n=4), apoptosis still spanned the entire brainstem; however, cells of the more lateral regions of the brainstem appeared to be spared as well as a thin region lining the medial ventricular surface (Figure 3-4B). This trend was seen again in the upper spinal cord, where apoptosis had spread to all but the most dorsal region of the spinal cord and the lower spinal cord, where apoptosis had begun to spread dorsally (Figure 3-4B).

The conditional deletion of Mcl-1 in the developing nervous system appeared to result in apoptosis that began in the rostral region of the brainstem and continued to spread caudally from E9 to E11 at each level; moreover, apoptosis spread from ventral to dorsal spanning most of the developing brainstem and spinal cord.

Figure 3-4. Apoptosis in the brainstem and spinal cord of Mcl-1 CKO embryos progresses in a rostral to caudal manner and within a section, from ventral to dorsal, over time. AC3 immunofluorescence (grey) was performed on brainstem and spinal cord section from **(A)** CTL and **(B)** Mcl-1 CKO littermates at E9, E10 and E11. Arrowheads indicate lateral and medial regions not immuno-positive for AC3.

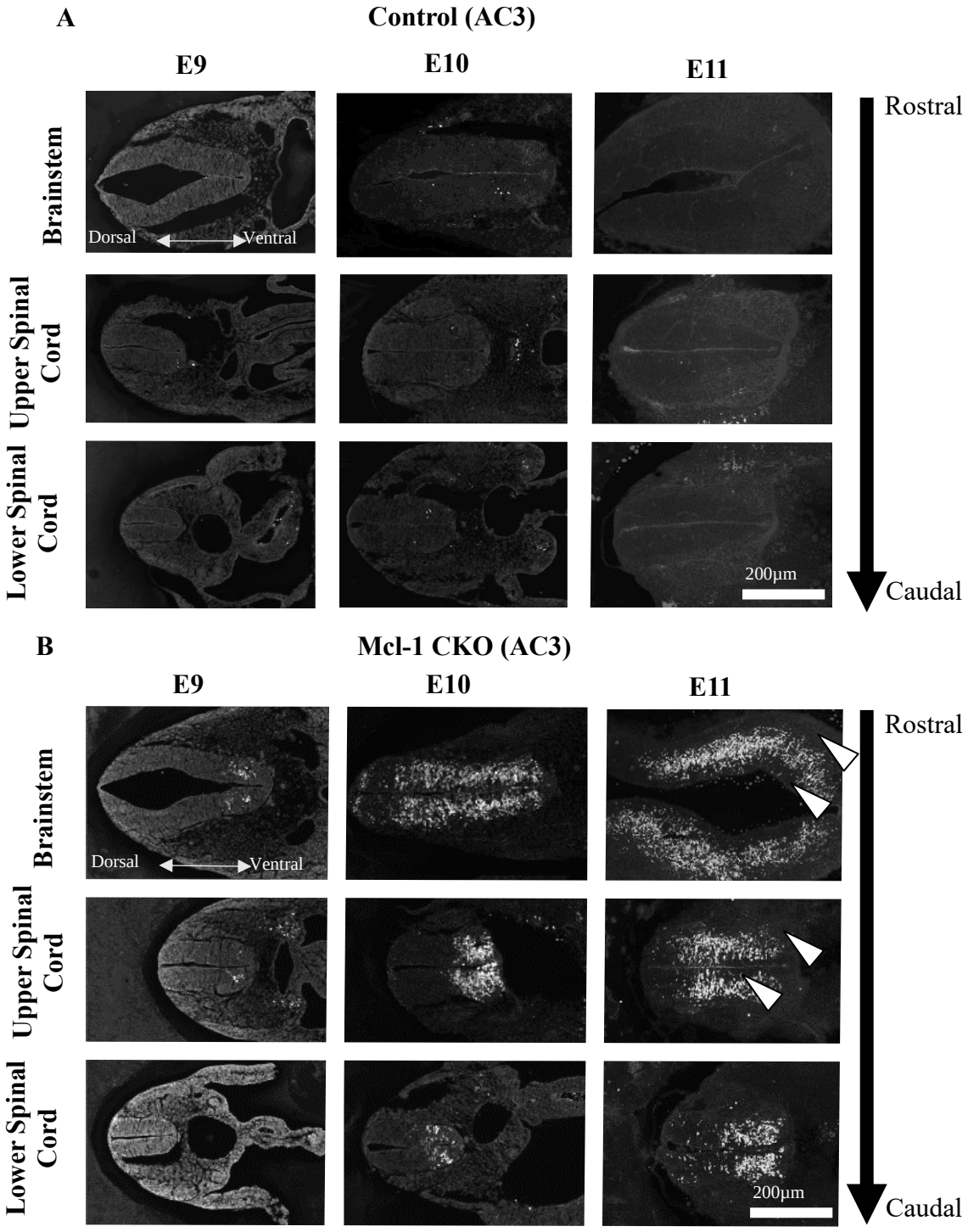
A
Control (AC3)
E9
E10
E11
Brainstem
Upper Spinal Cord
Lower Spinal Cord
Dorsal
Ventral
Rostral
Caudal
200µm
B
Mcl-1 CKO (AC3)
E9
E10
E11
Brainstem
Upper Spinal Cord
Lower Spinal Cord
Dorsal
Ventral
Rostral
Caudal
200µm

3-5 Apoptosis that occurs in Mcl-1 CKOs can be rescued through co-deletion of Bax.

The role that the anti-apoptotic Bcl-2 proteins have in preventing apoptosis is through the direct or indirect inhibition of Bax or Bak activation. To better understand the molecular pathway through which Mcl-1 inhibits apoptosis during developmental neurogenesis, Mcl-1 CKO mice were crossed with the BaxNull line of mice (Knudson et al., 1995). Bax was chosen as the likely effector protein responsible for apoptosis in the Mcl-1 CKO. Bax is expressed at E6 in early neural tissue whereas Bak is not expressed until E12 (Krajewska et al., 2002). The increase in apoptosis in the Mcl-1 CKO was seen prior to E12. Furthermore, no gross defects were observed in the nervous system of Bak Null mice (Lindsten et al., 2000). To investigate whether the co-deletion of Bax rescued apoptosis in the Mcl-1 CKO, the regions with the most extensive apoptosis, the ventral forebrain and dorsal spinal cord, were examined.

3-5-1 Apoptosis that occurs in ventral forebrain of the Mcl-1 CKO can be rescued through co-deletion of Bax.

To determine how Mcl-1 blocks apoptosis in the developing forebrain, immunofluorescence for AC3 was performed on E11 Mcl-1 CKO/BaxNull forebrains (Figure 3-5-1A). Forebrain sections of the Mcl-1 CKO/BaxNull double knockout revealed that co-deletion of Mcl-1 and Bax rescued the apoptosis that occurred in the E11 ventral forebrain of the Mcl-1 CKO alone. One-way ANOVA analysis of counts of AC3 immunofluorescence showed a main effect of genotype [$F(3,17)=36.45$, $p<0.0001$]. As expected, control and mice heterozygous for Mcl-1 and Bax (HET; image not shown) had little-to-no endogenous apoptosis in the ventral forebrains at E11 with CTL (n=5) and HETs (n=4) averaging 0.02% +/- 0.04% and 0.04% +/- 0.05% AC3 positive cells (Figure

3-5-1E). Using Hoechst staining, round, full nuclei could be observed (Figure 3-5-1b). Deletion of Mcl-1 in the Mcl-1 CKO (n=5) resulted in a significant increase in apoptosis with a mean percent AC3 positive cells of 31% +/- 10% in the ventral forebrain (Figure 3-5-1E, $p<0.0001$ compared to CTL, HET and Mcl-1 CKO/BaxNull using Tukey's multiple comparison test). Co-deletion of Mcl-1 and Bax (Mcl-1 CKO/BaxNull; n=4) resulted in a complete rescue of apoptosis in the ventral forebrain as seen by a lack of AC3 staining (2% +/- 2%; Figure 3-5-1 E), and by the presence of non-condensed, bright nuclei (Figure 3-5-1 d). Post-hoc analysis using Tukey's multiple comparison test showed no significant difference between % AC3 positive cells of CTL, HET or Mcl-1 CKO/BaxNull. The total number of cells within each area was counted and a one-way ANOVA revealed no significant main effect of genotype ($p=0.2584$; Figure 3-5-1 F).

Figure 3-5-1. Co-deletion of anti-apoptotic Mcl-1 and pro-apoptotic Bax rescues the apoptosis seen at E11 in Mcl-1 CKOs alone in the ventral forebrain. **(A)** Diagram of E11 embryo showing the location of the medial ganglionic eminence and the ROI where counts were performed. **(B, C, D)** Representative ventral forebrain sections where AC3 immunofluorescence (green) and Hoechst staining (grey) was performed. **(B, C, D)** Higher magnification of the 125µm x 125µm ROI where counts where performed. **(B, B')** CTL, **(C, C')** Mcl-1 CKO, and **(D, D')** Mcl-1 CKO/BaxNull. Arrowheads indicate where AC3 co-localizes with condensed nuclei (Hoechst). **(E)** Quantification of percent apoptotic cells. **(F)** Total number of nuclei. Analyses were performed using a one-way ANOVA. ***$p<0.0001$, error bars represent +/- SD.

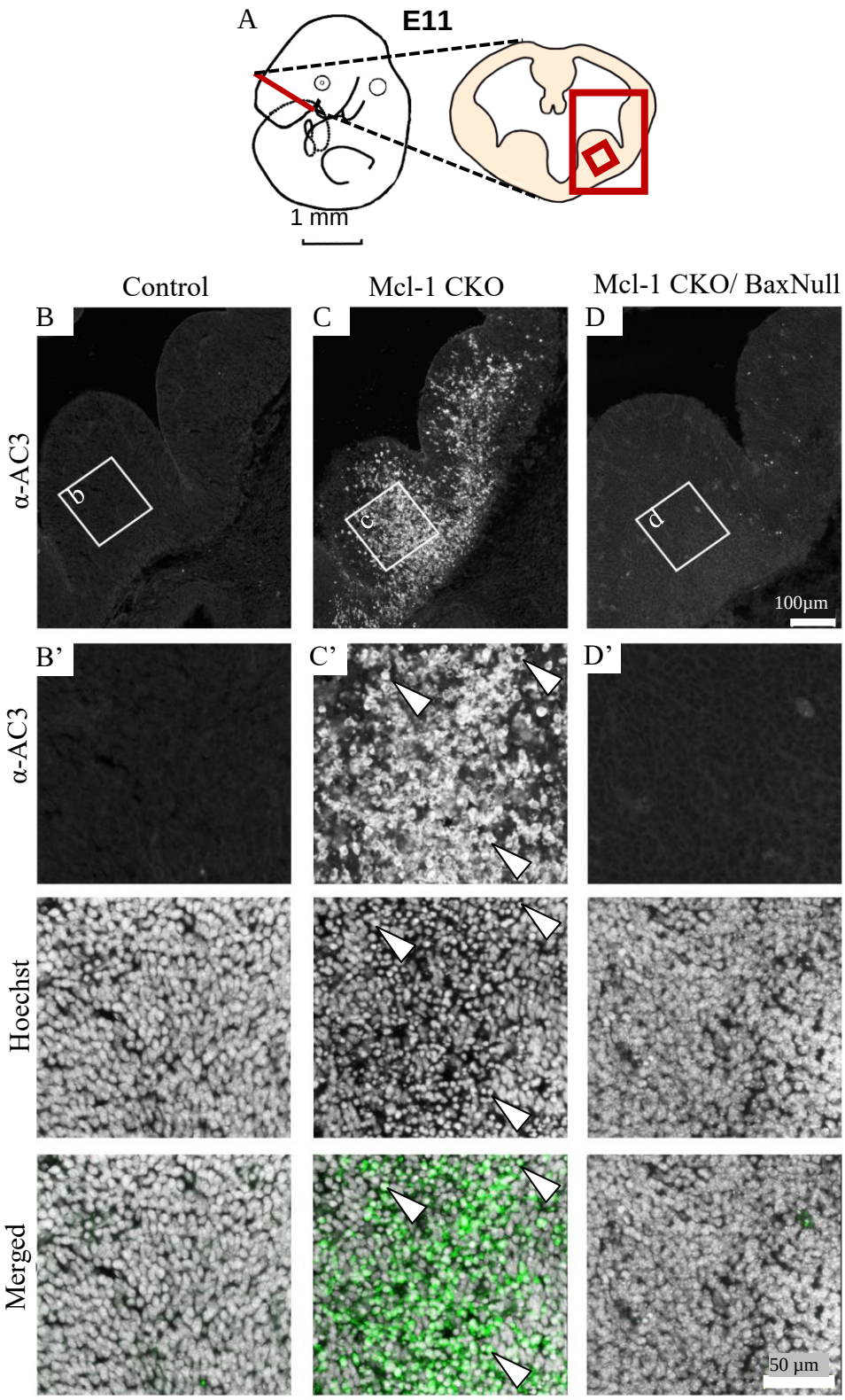
A
E11
1 mm
Control
Mcl-1 CKO
Mcl-1 CKO/ BaxNull
B
C
D
α-AC3
b
c
d
100µm
B'
C'
D'
α-AC3
Hoechst
Merged
50 µm

E

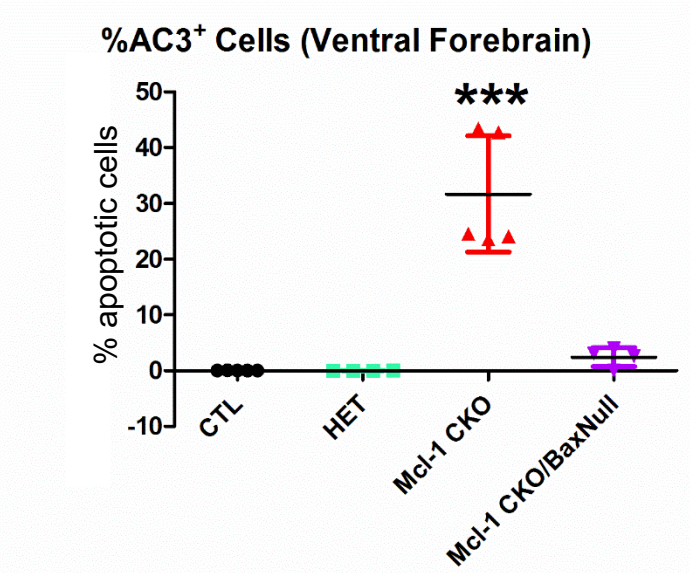
%AC3+ Cells (Ventral Forebrain)
% apoptotic cells
50
40
30
20
10
0
-10
***
CTL
HET
Mcl-1 CKO
Mcl-1 CKO/BaxNull

F

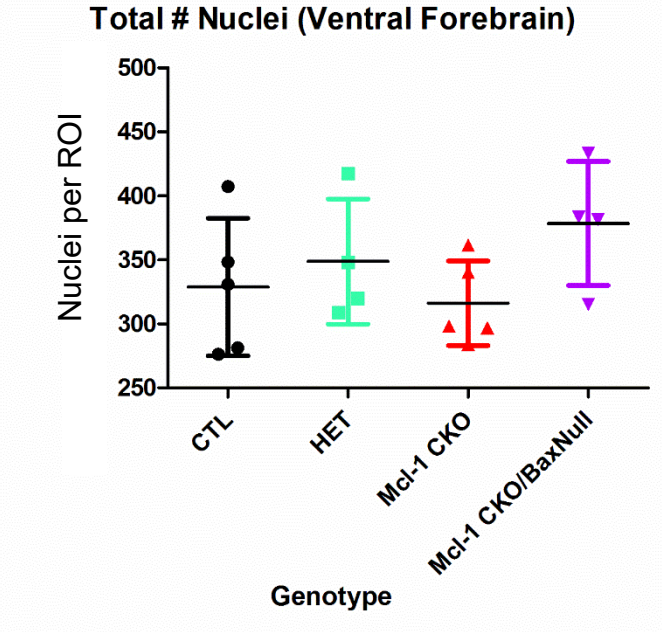
Total # Nuclei (Ventral Forebrain)
Nuclei per ROI
500
450
400
350
300
250
CTL
HET
Mcl-1 CKO
Mcl-1 CKO/BaxNull
Genotype

3-5-2 Apoptosis that occurs in the dorsal spinal cord of the Mcl-1 CKO can be rescued through co-deletion of Bax.

To determine if Mcl-1 prevents apoptosis through Bax inhibition in the spinal cord, apoptosis in Mcl-1 CKO/BaxNull cervical dorsal spinal cords was compared to the Mcl-1 CKO (Figure 3-5-2 A). Analysis using a one-way ANOVA of AC3 immunofluorescence counts combined with Hoechst nuclear staining of E11 spinal cord sections revealed a significant main effect of genotype [$F(3, 15) = 32.80$, $p<0.0001$]. Little apoptosis was observed in CTL (n=4) with mean of 0.06% +/- 0.12% apoptotic cells (Figure 3-5-2 B, E) and HET (n=5) with a mean of 0.06% +/- 0.14% apoptotic cells (image not shown; figure 3-5-2 E). As expected, Hoechst staining revealed round nuclei (Figure 3-5-2 B'). Mcl-1 CKO (n=4) spinal cords had a significant increase in apoptosis with a mean of 28% +/- 9.5% (Figure 3-5-2 C, C', E; $p<0.0001$ compared to CTL, HET and Mcl-1 CKO/BaxNull using Tukey's multiple comparison test). As with the ventral forebrain, Mcl-1 CKO/BaxNull double knock-outs showed a complete rescue of apoptosis in the dorsal spinal cord with a mean percent of 1.4% +/- 0.72% apoptotic cells (Figure 3-5-2 D, D', E). Post-hoc analysis using Tukey's multiple comparison test revealed no significant difference in apoptosis in CTL, HET and Mcl-1 CKO/BaxNull. One-way ANOVA analysis of the number of nuclei counted showed no significant difference between the number of nuclei counted in any of the four genotypes ($p=0.3874$; Figure 3-5-2 F).

Figure 3-5-2. Co-deletion of anti-apoptotic Mcl-1 and pro-apoptotic Bax rescues the apoptosis seen at E11 in the dorsal spinal cords of Mcl-1 CKOs. **(A)** Diagram of E11 embryo showing the location of the dorsal cervical spinal cord and the ROI where counts were performed. **(B, C, D)** Representative dorsal cervical spinal cord sections where AC3 immunofluorescence (green) and Hoechst staining (grey) were performed. **(B', C', D')** Higher magnification of the 125µm x 125µm ROI where counts were performed. **(B, B')** CTL, **(C, C')** Mcl-1 CKO, and **(D, D')** Mcl-1 CKO/BaxNull. Arrowheads indicate where AC3 colocalizes with condensed nuclei (Hoechst). **(E)** Quantification of percent apoptotic cells. **(F)** Total number of nuclei. Analyses were performed using a one-way ANOVA. ***$p<0.0001$, error bars represent +/- SD.

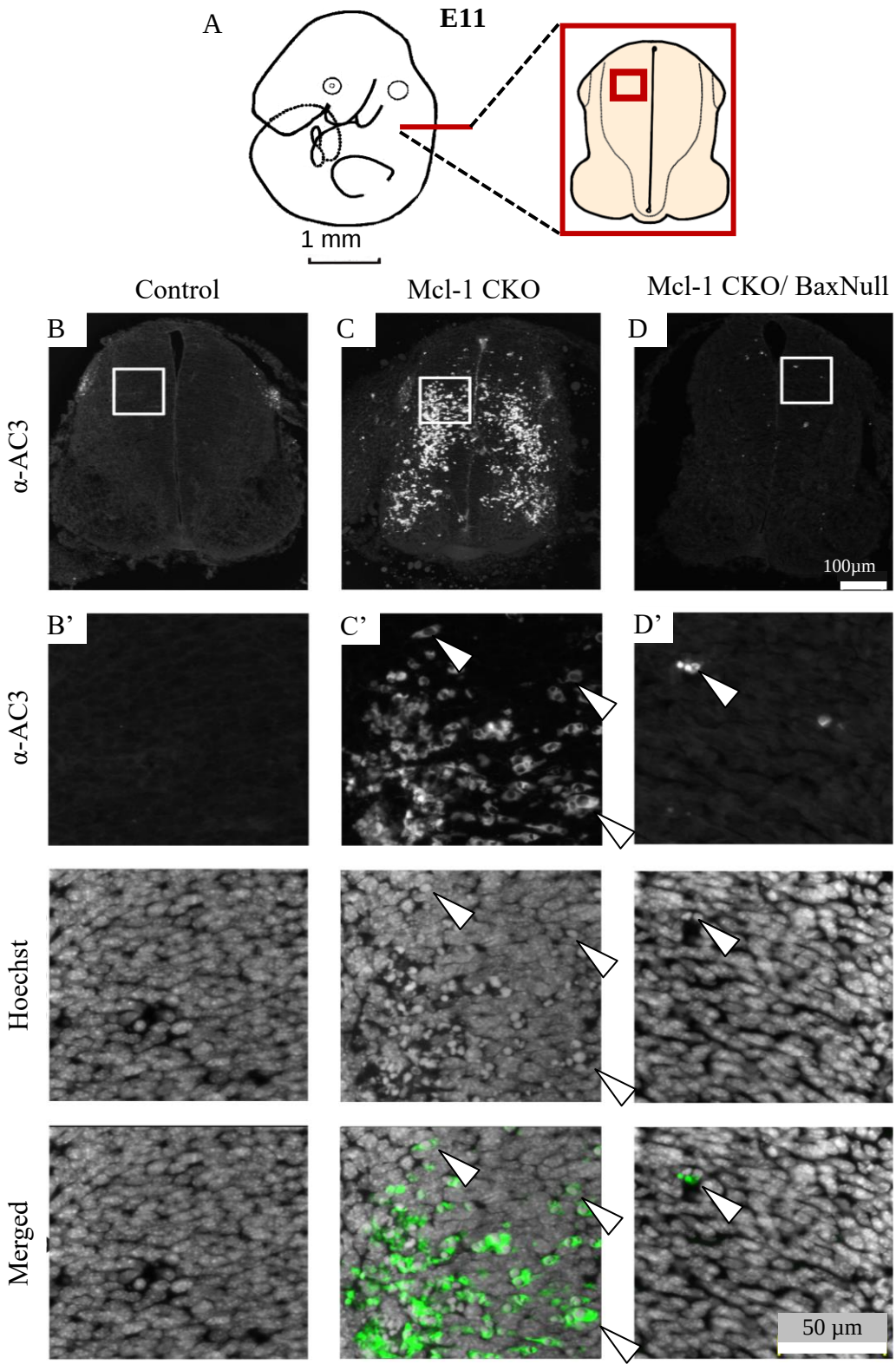
A
E11
1 mm
Control
Mcl-1 CKO
Mcl-1 CKO/ BaxNull
B
C
D
α-AC3
100µm
B'
C'
D'
α-AC3
Hoechst
Merged
50 µm

E

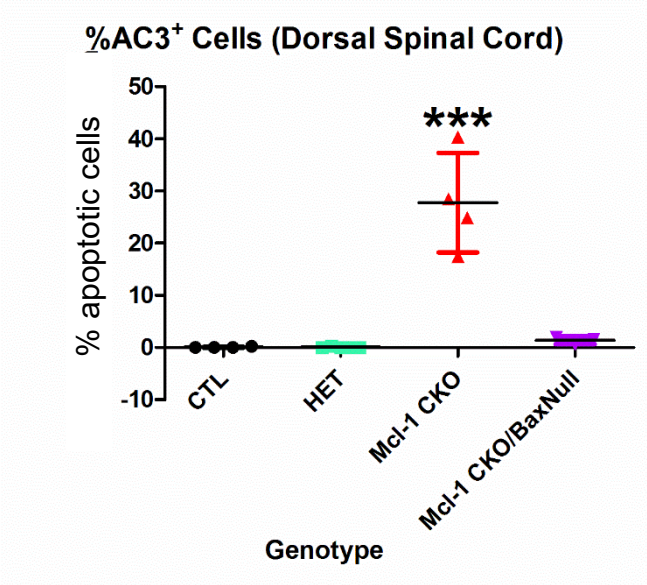
%AC3+ Cells (Dorsal Spinal Cord)
% apoptotic cells
50
40
30
20
10
0
-10
***
CTL
HET
Mcl-1 CKO
Mcl-1 CKO/BaxNull
Genotype

F

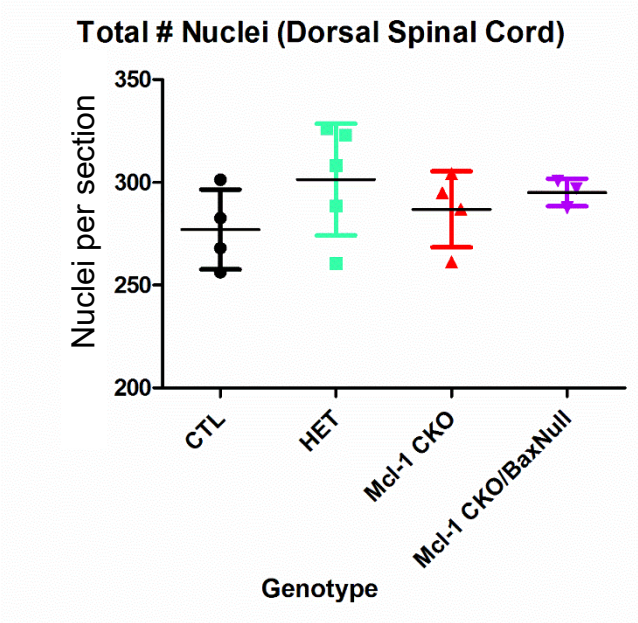
Total # Nuclei (Dorsal Spinal Cord)
Nuclei per section
350
300
250
200
CTL
HET
Mcl-1 CKO
Mcl-1 CKO/BaxNull
Genotype

3-5-3 Co-deletion of Mcl-1 and Bax does not rescue all apoptosis throughout the brainstem and spinal cord of the developing nervous system at E11.

To determine whether co-deletion of Bax rescued apoptosis throughout the entire developing nervous system, AC3 immunofluorescence was performed on brainstem and further spinal cord sections (Figure 3-5-3A). This revealed that although apoptosis was completely rescued in the dorsal spinal cord at E11 in the Mcl-1 CKO/BaxNull, there were regions throughout the developing nervous system that were incompletely rescued. Few apoptotic cells were observed in the CTL (n=4) brainstem and spinal cord as previously demonstrated. Apoptosis was extensive in the Mcl-1 CKO (n=4), with a dorsal to ventral progression across the section and in a rostral to caudal manner. In the Mcl-1 CKO/BaxNull embryo (n=3), apoptosis appeared to be rescued in the cervical and lumbar sections of the spinal cord; however, there were still apoptotic cells in the ventral thoracic spinal cord (Figure 3-5-3D'). In the brainstem, most of the apoptosis in the Mcl-1 CKO/BaxNull co-deletion model was rescued, except in the dorsomedial region (Figure 3-5-3B'). This suggested that although *mcl-1* and *bax* co-deletion rescued most apoptosis associated with the Mcl-1 CKO, this rescue was incomplete.

Figure 3-5-3. Co-deletion of Mcl-1 and Bax does not rescue all apoptosis throughout the developing nervous system at E11. **(A-E)** Diagram of E11 embryo showing the levels of the brainstem and spinal cord where AC3 immunofluorescence (grey) was performed. Representative sections of **(B')** brainstem, **(C')** cervical spinal cord, **(D')** thoracic spinal cord and **(E')** lumbar spinal cord of CTL, Mcl-1 CKO and Mcl-1 CKO/BaxNull. Arrowheads indicate where apoptosis is not rescued in Mcl-1 CKO/BaxNull embryos.

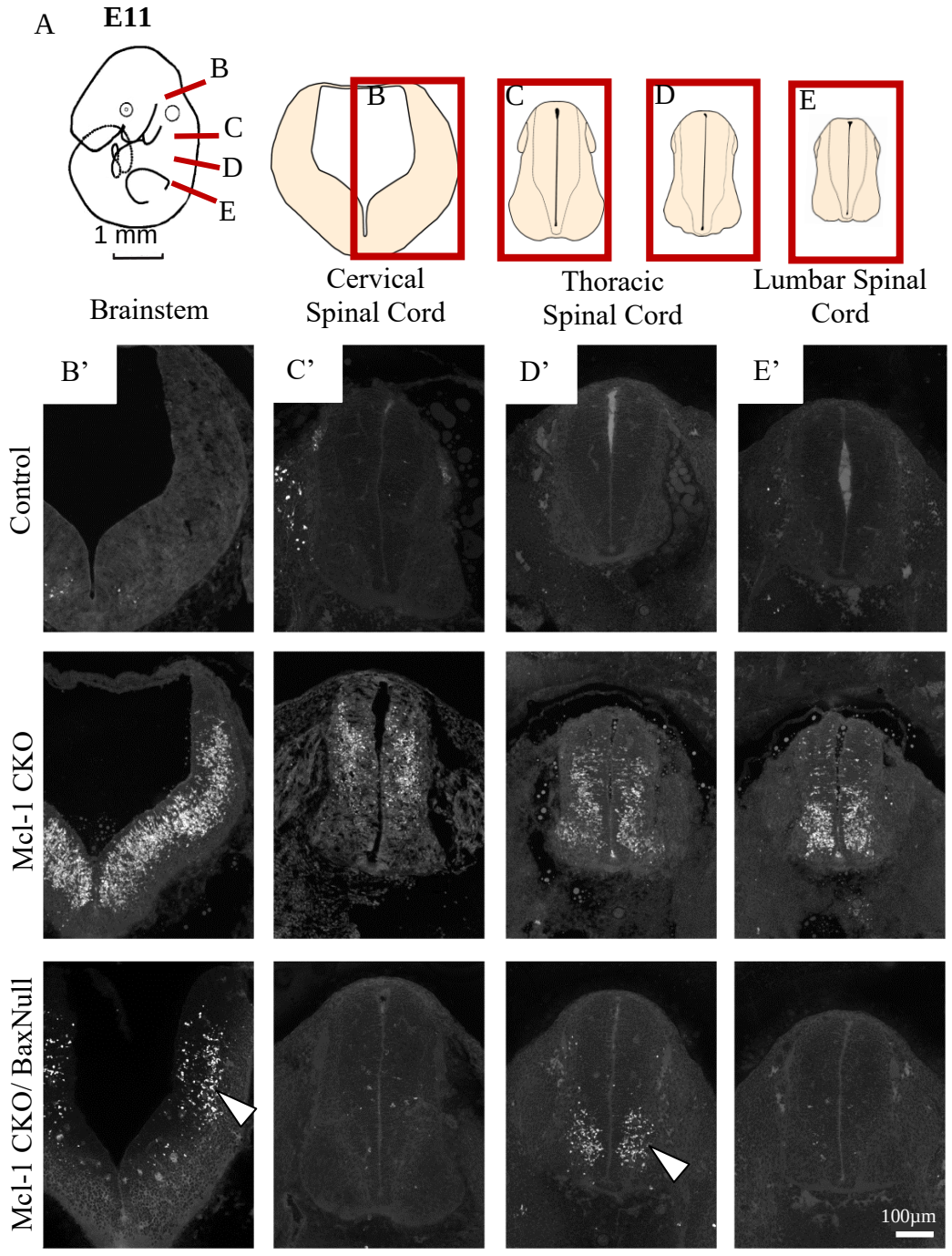
A
E11
B
C
D
E
1 mm
Brainstem
Cervical Spinal Cord
Thoracic Spinal Cord
Lumbar Spinal Cord
B'
C'
D'
E'
Control
Mcl-1 CKO
Mcl-1 CKO/ BaxNull
100µm

3-5-4 Apoptosis is rescued throughout the developing brain of E11 Mcl-1 CKO embryos when Bax is co-deleted.

To see if the incomplete rescue in the Mcl-1 CKO/BaxNull model seen in the spinal cord was also found throughout the developing brain, AC3 immunostaining of brain sections of CTL (n=4), Mcl-1 CKO (n=4), and Mcl-1 CKO/BaxNull (n=4) E11 brain was performed. In contrast to the brainstem and spinal cord, apoptosis appeared to be completely rescued throughout the rostral to caudal regions of the brain. The lateral regions of the medial and lateral ganglionic eminence had a few AC3 positive cells, as did the dorsal-medial forebrain (Figure 3-5-4C), which may indicate a lack of complete rescue, but no region appeared to have any large clustering of apoptotic cells as observed in the brainstem and spinal cord (Figure 3-5-3). This indicated that throughout the developing brain, Mcl-1 is needed to prevent Bax-mediated apoptosis.

Figure 3-5-4. Apoptosis is rescued throughout the developing brains of E11 Mcl-1 CKO embryos when Bax is co-deleted. E11 brain sections of **(A)** CTL **(B)** Mcl-1 CKO and **(C)** Mcl-1 CKO/BaxNull immunostained for AC3 (grey). Arrowheads indicate regions where there was an occasional apoptotic cell.

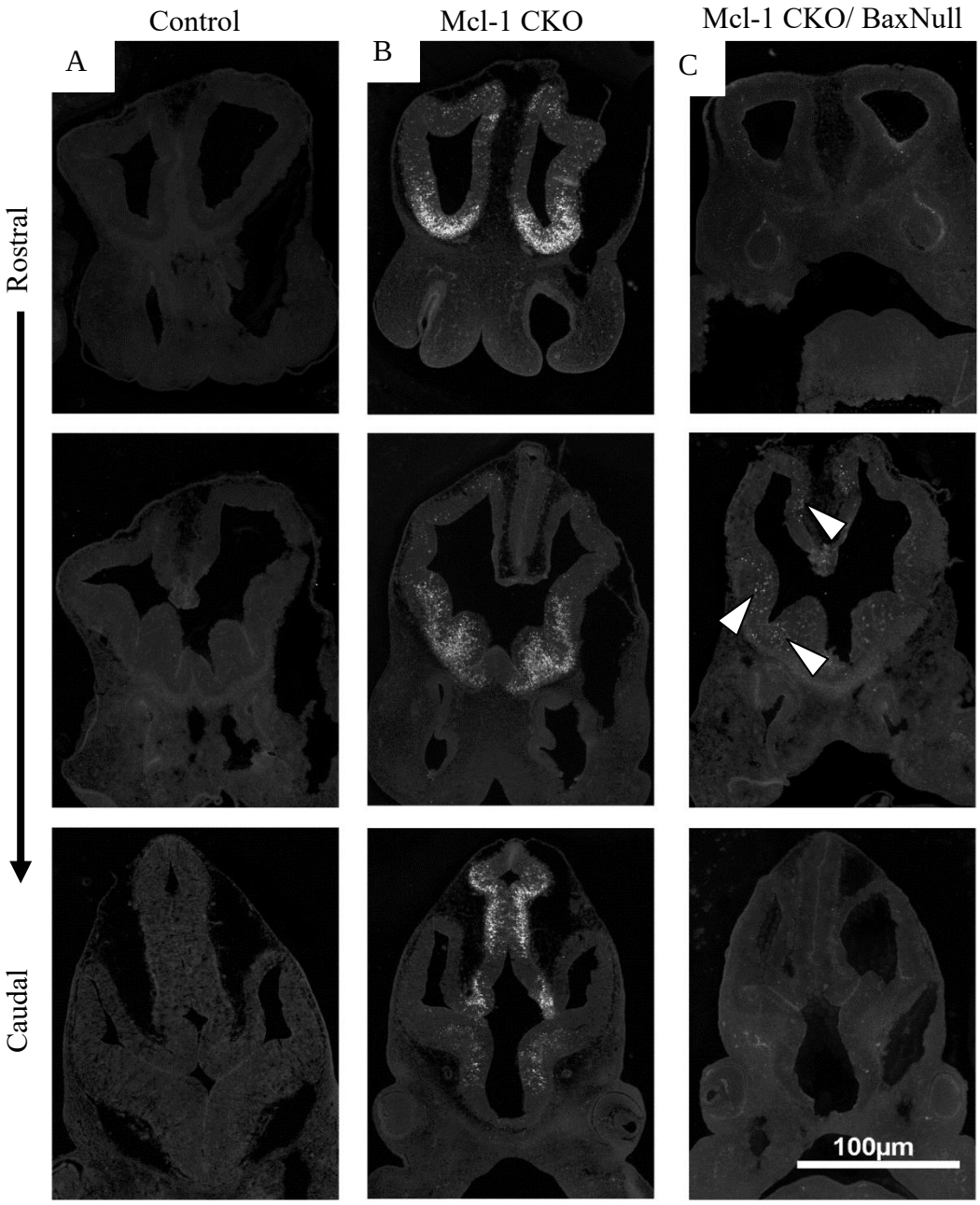
Control
Mcl-1 CKO
Mcl-1 CKO/ BaxNull
A
B
C
Rostral
Caudal
100µm

3-6 Apoptosis in differentiating Mcl-1 CKOs was rescued through co-deletion of Bax *in vitro.*

The *in vivo* results show apoptosis in the Mcl-1 CKO begins with the onset of neurogenesis, when differentiation begins. I next investigated whether NPCs became dependent on Mcl-1 for survival as they differentiate *in vitro*. To address this, neurospheres were induced to differentiate for 1, 3 or 7 days. Immunocytochemistry for AC3 was performed and apoptotic cells were counted (Figure 3-7A). Using a two-way ANOVA, a significant main effect of interaction was found [$F(6,45) = 3.949$, $p<0.01$], a main effect of genotype was found [$F(3,45) = 24.19$, $p<0.0001$], but no main effect of time ($p=0.3954$) was found. Bonferroni post-hoc analysis at day 1 revealed Mcl-1 CKOs had significantly more apoptosis compared to both BaxNull ($p<0.05$) and Mcl-1 CKO/BaxNull ($p<0.05$). There was no significant difference between CTL and BaxNull, Mcl-1 CKO or Mcl-1 CKO/BaxNull. At day 3 Mcl-1 had significantly more apoptosis than BaxNull ($p<0.01$). There was no significant difference between CTL and either BaxNull, Mcl-1 CKO or Mcl-1 CKO/BaxNull. Increased apoptosis was observed in Mcl-1 CKOs at day 7 compared to CTL ($p<0.001$) and BaxNull cells ($p<0.001$), and this increase was abolished when *bax* was co-deleted (Figure 3-7B; $p<0.001$). This showed that NPCs are dependent on Mcl-1 for survival *in vitro* as they differentiate and that co-deletion of *bax* can rescue the apoptosis seen in Mcl-1 CKOs alone.

Figure 3-6. Differentiation of neurospheres *in vitro* causes apoptosis in Mcl-1 CKOs and this is rescued in Mcl-1 CKO/BaxNulls. Neurospheres were cultured from E11 forebrains for 3 days *in vitro* before differentiating. **(A)** Representative images of day 7 *in vitro* differentiated neurospheres reveal increases in AC3 staining (green) in Mcl-1 CKOs compared to CTLs was rescued in the Mcl-1 CKO/BaxNull double knock-out. White arrowheads indicate examples of AC3 staining. Hoechst staining shows nuclei (grey). **(B)** Quantification of percent AC3 positive cells. Statistical analysis was carried out using a two-way ANOVA with Bonferroni post-hoc. ***$p<0.0001$, error bars represent +/- SD.

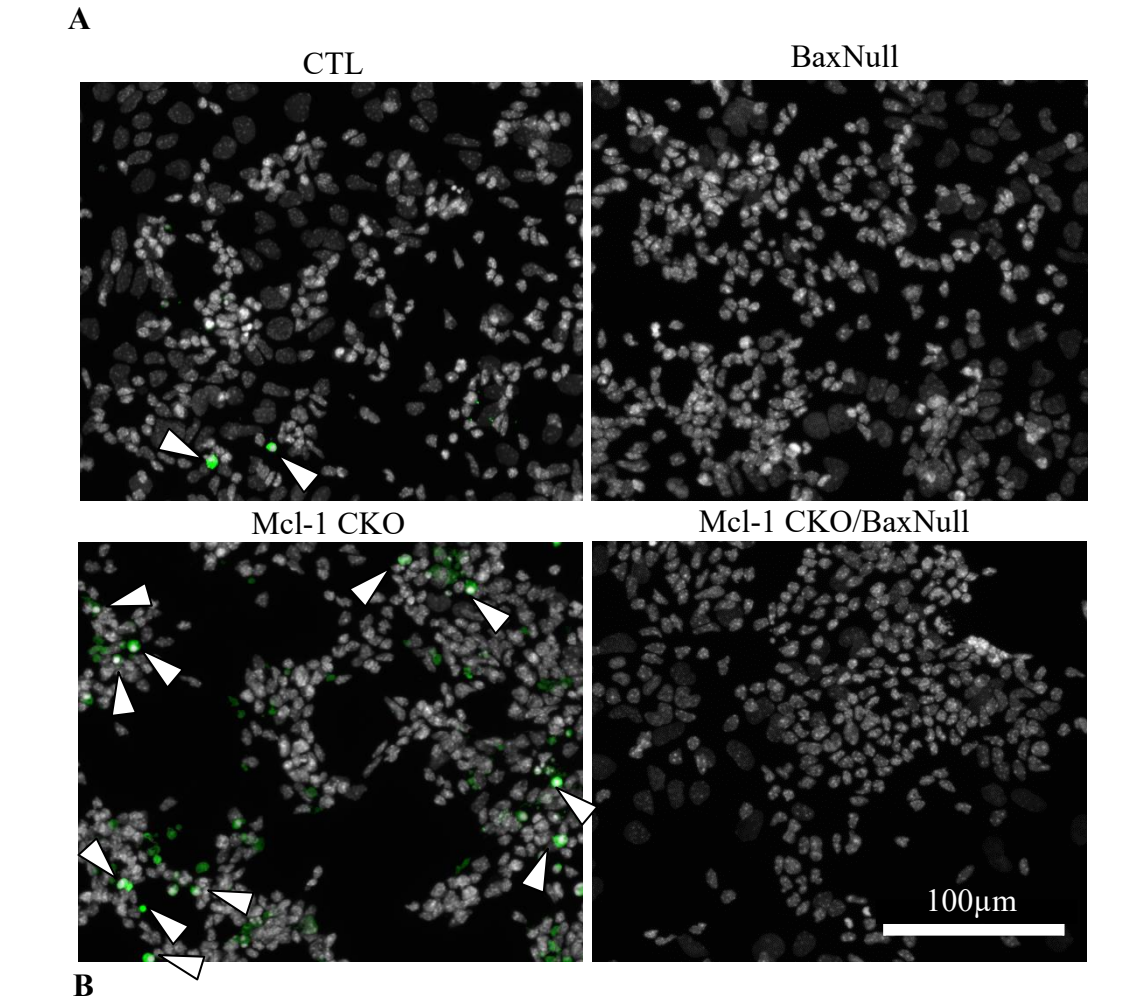
A
CTL
BaxNull
Mcl-1 CKO
Mcl-1 CKO/BaxNull
100µm
B
AC3
% AC3+
20
15
10
5
0
*
*
**
***
Day 1
Day 3
Day 7
Timepoint
CTL
BaxNull
Mcl-1 CKO
Mcl-1 CKO/BaxNull

3-7 Co-deletion of Mcl-1 and Bax was embryonic lethal in one transgenic model, but not another.

Mcl-1 CKOs have been found to be lethal by E15.5 (Arbour et al., 2008). As the Mcl-1 CKO/BaxNull rescued the majority of apoptosis associated with Mcl-1 CKO alone, the survival rate of these embryos was investigated to see if the double knockout rescued the embryonic lethality. As shown in Table 3.1, at E11 the Mcl-1 CKO/BaxNull co-deletion model survives at a rate predicted by Mendelian genetics, but it is embryonic lethal by E13. In contrast, when Mcl-1 CKO mice containing one floxed allele of *bax* and one null allele of *bax* (NesCre:Mcl-$1^{f/-}$:$Bax^{f/-}$; Mcl-1 CKO/BaxNull:Floxed) were generated, they survived to at least postnatal day 18 (P18). P18 was the latest timepoint investigated (Table 3.2).

Table 3.1: Recovery of Mcl-1 CKO/BaxNull embryos.

Mcl-1 CKO/BaxNull	Embryonic Time Point		
	E11	E12	E13
Number of litters	18	2	16
Number of embryos	182	14	136
Number of knock-outs (%)	14 (7.7%)	1 (7.1%)	1 (0.7%)
Predicted number with Mendelian ratio (%)	11 (6.25%)	1 (6.25%)	7 (5.31%)

Table 3.2: Recovery of Mcl-1 CKO/BaxNull:Floxed embryos.

Mcl-1 CKO/ BaxNull:Floxed	Embryonic Time Point				
	E11	E12	E13	E15	P18
Number of litters	6	2	1	1	1
Number of embryos	62	11	8	10	9
Number of knock-outs (%)	6 (9.7%)	2 (18%)	1 (12.5%)	3 (30%)	2 (22%)
Predicted number with Mendelian ratio (%)	6 (8.87%)	1 (6.25%)	2 (25%)	3 (25%)	2 (25%)

4-0 Discussion

The experiments performed in this thesis investigated the anti-apoptotic role that Mcl-1 has in the formation of the early murine nervous system *in utero.* Using the Mcl-1 CKO model, several novel functions of Mcl-1 have been elucidated. First, Nestin:Cre-mediated *mcl-1* deletion resulted in apoptosis throughout the forebrain, brainstem and spinal cord of the developing nervous system. Second, co-deletion of *mcl-1* and *bax* revealed that the pro-survival role of Mcl-1 is largely through pro-apoptotic Bax in both the forebrain and spinal cord. Last, *in vitro* modeling of NPCs using neurospheres showed differentiating NPCs depend on Mcl-1 for survival. Collectively, these results suggest a pan-nervous system dependency on Mcl-1 during development for survival through inhibition of pro-apoptotic Bax.

4-1 Dependency on Mcl-1 is widespread in the developing nervous system.

Mcl-1 expression has been found in the early implanting embryo, with expression peaking at E5, and decreasing slightly at E6.5 (Rinkenberger et al., 2000). Germline deletion of *mcl-1* is preimplantation lethal at E3.5-E4, suggesting a critical role for Mcl-1 in early embryonic development (Rinkenberger et al., 2000). Expression of Mcl-1 has also been found at E10, E11.5, E12 and E15.5 in the developing forebrain (Arbour et al., 2008; Fogarty et al., 2018). No study has investigated the onset of Mcl-1 expression in the developing nervous system. Formation of the neural tube from the neural plate begins at E8, so this time point was investigated to determine if Mcl-1 expression was present in the early developing nervous system (Copp et al., 2003). As Mcl-1 is found in the embryo at E6 and E10, it was hypothesized that Mcl-1 protein is expressed in between these

timepoints. Western blot analysis revealed Mcl-1 is expressed at E8 in the embryonic heads. Due to the small size of the E8 embryo, contaminating tissue from outside of the nervous system prevents a conclusive argument that Mcl-1 is present at E8 in the developing nervous system. A lack of an effective antibody or riboprobe for tissue histology limits the analysis to Western blotting.

The complete deletion of Mcl-1 in the Mcl-1 CKO model used in this thesis has been shown in the E12 forebrain, brainstem and spinal cord, but not at an earlier timepoint (Fogarty et al., 2018). As the aims of this thesis were to investigate the role Mcl-1 plays in the survival of the early nervous system, the effective deletion of Mcl-1 at earlier timepoints needed to be addressed. The Mcl-1 CKO uses Nestin-mediated:Cre to selectively delete both alleles *mcl-1* in NPCs (Arbour et al., 2008). Expression of Nestin begins at E7.5 and can be found in proliferating populations throughout the early nervous system, apart from the olfactory epithelium and hippocampal granule neuron progenitor populations (Dahlstrand et al., 1995; Kawaguchi et al., 2001). Effective Cre expression in the Nestin:Cre embryo has been shown using β-galactosidase staining of a Rosa LacZ reporter mouse at E12.5 (Bérubé et al., 2005); however, deletion of *mcl-1* prior to E12 has not been examined in the Mcl-1 CKO. Western blot analysis of E10 Ctl vs Mcl-1 CKO forebrain, brainstem and spinal cord show that only in the forebrain is Mcl-1 significantly reduced, although a non-significant, trending decrease is observed with the brainstem and spinal cord. As with the E8 nervous system tissue, limitations in the dissection cannot preclude contaminating, non-neural tissue. Another limitation could be the small sample size. As there was a strong trend towards a decrease in Mcl-1 in the brainstem, increasing the sample size could have resulted in significance.

Cre inducible deletion is not always complete (Chen et al., 2016; Liang et al., 2012). The Nestin:Cre mice in the study were developed by Bérubé et al (2005). Cre expression was shown by E12 in these mice. Although it is plausible that Mcl-1 is not completely knocked out at E8-E11, it has been shown that Mcl-1 is completely knocked-out in forebrains, brainstems and spinal cords of mice at E12, suggesting the deletion of Mcl-1 in the nervous system is complete (Fogarty et al., 2018). One limitation of this study is that complete deletion of a gene using Nestin:Cre has not been shown at a timepoint earlier than E12.

The Mcl-1 CKO has previously been shown to result in embryonic lethality by E15.5 (Arbour et al., 2008). Apoptosis in the Mcl-1 CKO has been found in the developing forebrain at E12.5 and was observed in $Nestin^+$ NPCs, $Doublecortin^+$ migrating neuroblasts and $Tuj1^+$ newly born neurons (Arbour et al., 2008). Apoptosis prior to E12.5 in the forebrain had not been investigated. Apoptosis was first seen in the ventral forebrain at E10, but not prior, at E9. This indicates that, in the Mcl-1 CKO, apoptosis initiates in ventral forebrain at E10. This region of the forebrain consists of the early medial and lateral ganglionic eminences, which contain precursors to the subpallial regions of the brain, as well as cortical GABAergic interneuron precursors (Lavdas et al., 1999; Turrero Garcia & Harwell, 2017). The continued widespread apoptosis in the ventral E11 forebrain suggests that many precursor populations are dependent on Mcl-1 for survival.

The dependency of precursor populations on Mcl-1 within the developing brainstem and spinal cord has not previously been investigated. Apoptosis started in the ventral brainstem at E9 and then, over time from E9 to E11, spreads across two axes,

from ventral to dorsal as well as from rostral to caudal. This progression closely mirrors the differentiation of the developing spinal cord and brainstem. Differentiation in the developing spinal cord begins ventrally and progresses dorsally (McConnell, 1981). Further, rostral signalling with RA from the somatic mesoderm causes cells of the developing neural tube to differentiate, whereas caudal Wnt and Fgf signalling prevents differentiation. This results in a progression of differentiation that begins rostrally and progresses caudally over time (Gouti et al., 2015). The similarity between the progression of apoptosis in the Mcl-1 CKO and the progression of differentiation in the developing spinal cord suggests that NPCs in the developing nervous system may become dependent on Mcl-1 as they differentiate. Mcl-1 has been shown to be an important survival factor as NPCs of the developing forebrain differentiate into immature neurons (Arbour et al., 2008). Further, Mcl-1 has been identified as an important factor in the terminal mitosis of NPCs as they differentiate into post-mitotic neurons (Hasan et al., 2013).

Patterning of the spinal cord begins at E9.5 and the many types of neurons within the adult spinal cord are derived from twelve basic progenitor cell types (Alaynick et al., 2011). The progression of apoptosis in the Mcl-1 CKO across the developing spinal cord and brainstem appears to affect most cell populations showing that many precursor populations are dependent on Mcl-1 for survival. Interestingly, apoptosis does not occur immediately adjacent to the midline of the spinal cord and brainstem. The midline is where actively dividing cells are located, and previous research in the forebrain has shown that Phospho-Histone H3 positive cells, cells that are in mitosis, do not change in number in the Mcl-1 CKO (Arbour et al., 2008). Another region spared from apoptosis is the ventral horns of the developing spinal cord. Although not quantified, some cells in the

ventral horns at E11 undergo apoptosis in the Mcl-1 CKO, but most cells are spared. The ventral horns contain motor neurons. This region has been shown to be dependent on Bcl-xL, another anti-apoptotic Bcl-2 family member that may compensate for the loss of Mcl-1 in the Mcl-1 CKO (Fogarty et al., 2018; Fogarty et al., 2016).

An interesting observation in the Mcl-1 CKO is that the early nervous system still forms. This implies that the early nervous system is not dependent on Mcl-1 for survival and that NPCs in the developing nervous system acquire a dependency on Mcl-1.

The absence of Mcl-1 appears to trigger apoptosis without any additional stimulus. This suggests that NPCs of the developing nervous system are primed to die. These cells may require constant pro-survival signalling to prevent apoptosis. It has been observed that human embryonic stem cells are primed to die, as well, with a large amount of pro-apoptotic PUMA being expressed and relatively lower expression of anti-apoptotic Bcl-2. This primed state is not observed in more differentiated cells (Geijsen, 2013; Liu et al., 2013). This could be the case with the cells of the nervous system, where a large amount of pro-apoptotic signalling is constantly present in NPCs. As was seen in the differentiating embryonic stem cells, as NPCs differentiate into mature neurons, their dependency on Mcl-1 is not anti-apoptotic in nature, and deletion of *mcl-1* no longer results in increased apoptosis, but autophagy (Germain et al., 2011). Mature, adult neurons become resistant to apoptosis partially through inhibition of PUMA and BIM by microRNAs as well as inhibition of APAF1, increased expression of XIAP and decreased expression of AC3 (Annis et al., 2016; Kristiansen & Ham, 2014).

4-2 Mcl-1 exerts its pro-survival function through inhibition of Bax activation.

The Bcl-2 family contains pro-apoptotic and anti-apoptotic members that act to inhibit each other. The BH3-only proteins act as sensors, detecting damage and death signals within the cell. Upon activation, they activate the effector proteins Bax and/or Bak. The anti-apoptotic Bcl-2 family members, including Mcl-1, inhibit both the BH3-only members and the effector proteins (Youle & Strasser, 2008). No research has elucidated the pro-apoptotic effector protein that Mcl-1 acts to inhibit in the developing nervous system. There are two pro-apoptotic effector proteins, Bax and Bak. Bax was the first candidate as it has been associated with being inhibited by Mcl-1 (Germain et al., 2008). Further, Bax has been shown to be important in promoting cellular death in nervous system development (Deckwerth et al., 1996; Vekrellis et al., 1997). In contrast, Bak deficient mice have not been shown to have gross nervous system dysfunction (Lindsten et al., 2000). A co-deletion model of Mcl-1 and Bax was generated by crossing the Mcl-1 CKO onto a BaxNull line of mice. Of note, there was no significant differences in the number of nuclei in the CTL, Mcl-1 CKO, and Mcl-1 CKO/BaxNull. This means the apoptosis in the Mcl-1 CKO was recent, as there had not been time to clear the nuclei that have condensed as the cells underwent apoptosis (Bursch et al., 1990). Apoptosis in the Mcl-1 CKO is rescued through co-deletion of *bax* in both the ventral forebrain and the dorsal cervical spinal cord. Observations of the entire spinal cord and forebrain reveal that although most of the apoptosis in the Mcl-1 CKO/BaxNull mouse model is rescued compared to the Mcl-1 CKO alone, certain regions appear to not be rescued. These regions contain clustering of AC3 positive cells within the dorso-medial brainstem and

the ventral lumbar region of the spinal cord. The brain of the double knockout does not contain any large clustering of AC3 positive cells, but a few are found in the lateral regions of the medial and lateral ganglionic eminences. These regions of incomplete rescue may be dependent on Mcl-1 directly or indirectly interacting with Bak to prevent apoptosis.

The complete pathway of how Mcl-1 inhibits apoptosis has yet to be elucidated; however, the experiments presented show that Mcl-1 acts to prevent Bax from initiating apoptosis, whether it be direct or indirect. Mcl-1 could directly interact with Bax, or it could bind and inhibit a BH3-only protein. Whether inhibited directly or indirectly, Bax needs to be activated by a BH3-only protein to initiate apoptosis (Youle & Strasser, 2008). The candidates through which Mcl-1 inhibits Bax are the BH3-only proteins. To prevent the activation of Bax, Mcl-1 would need to prevent a direct-activator BH3-only protein from binding and activating Bax. The two direct activators that have been shown to interact with Mcl-1 are Bim and PUMA (Shamas-Din et al., 2013). Previous data from our lab suggests that Bim expression is high in the developing nervous system, making it the likely candidate, yet co-deletion of Mcl-1 and Bim in T-lymphocytes was unable to rescue the apoptosis induced by deletion of Mcl-1 alone (Tripathi et al., 2013). An alternative hypothesis is that Mcl-1 blocks both Bim and PUMA in the T-lymphocytes, and this could be true for the developing nervous system as well. Co-deletion of Bim and Bcl-xL rescues the apoptosis associated with deletion of Bcl-xL alone in hematopoietic cells but does not rescue apoptosis in the developing nervous system, suggesting that more pro-apoptotic proteins may be important in the nervous system (Akhtar et al., 2008). PUMA has been found to be important for promoting death after gamma

irradiation in the adult brain (Jeffers et al., 2003). In embryonic NPCs, PUMA deletion prevents death due to genotoxic stress (Akhtar et al., 2006). These findings suggest that PUMA is at least partially responsible for apoptosis in the nervous system, although future studies would be required to determine if Mcl-1 is responsible for inhibiting the pro-apoptotic activity of PUMA.

4-3 *in vitro* analysis reveals the pro-survival role of Mcl-1 may vary depending on the state of differentiation.

In vitro analysis of primary cell cultures allows more precise control over the conditions in which cells grow. Using neurosphere cultures derived from NPCs of the developing E11 forebrain, one can maintain cells in a proliferative state and inhibit differentiation from occurring (Reynolds & Weiss, 1992). Upon coating the cell culture dishes and the addition of a differentiating media containing FBS, neurospheres begin to adhere to the dish and differentiate. In Mcl-1 CKO differentiating neurospheres, it took seven days for apoptosis to significantly increase. This suggests that as NPCs differentiate, they acquire a dependency on Mcl-1 for survival.

The 7 days it took for apoptosis to occur in the differentiating Mcl-1 CKOs could be due to cells lifting off as they undergo apoptosis. At earlier timepoints, when the neurospheres are less differentiated, they are less adhered to the culture dishes. Cells naturally lift off dishes and separate from other cells when they undergo apoptosis. As cells differentiate, they become more adherent to the dish. Cells undergoing apoptosis prior to day 7 may lift off faster and wash away during immunocytochemistry, artificially

masking an increase in apoptosis at earlier timepoints. Importantly, however, the Mcl-1 CKO/BaxNull co-deletion model was able to rescue the increased apoptosis seen in the Mcl-1 CKO alone *in vitro* showing that the rescue effect is cell autonomous.

4-4 Co-deletion of Mcl-1 and Bax was embryonic lethal in one transgenic model, but not in another.

The co-deletion of Mcl-1 and Bax rescued apoptosis but did not initially appear to rescue embryonic lethality. This was using the Mcl-1 CKO/BaxNull mouse line ($Nes:Cre^{+/-}$:$Mcl\text{-}1^{f/f}$:$Bax^{-/-}$) where there is embryonic lethality prior to E13. This is unusual as the Mcl-1 CKO is embryonic lethal at E15.5 (Arbour et al., 2008) and Bax Null mice are not embryonic lethal, but instead survive to adulthood (Knudson et al., 1995). When one Bax Null allele was switched for a Bax floxed allele ($Nes:Cre^{+/-}$:$Mcl\text{-}1^{f/f}$:$Bax^{-/f}$) however, the embryonic lethality was rescued and pups survived beyond birth to, at least, postnatal day 18. It is counterintuitive that swapping a single Bax Null allele with a Bax floxed allele would rescue the embryonic lethality. Other unknown genetic defects in the transgenic line could be to blame for the inability of the Mcl-1 CKO/BaxNull mice to survive to birth.

4-5 Future directions

The work presented highlights the role that Mcl-1 plays in the early development of the nervous system; however, more experiments are needed to fully understand the role of Mcl-1 in neurogenesis.

Firstly, Mcl-1 expression appears to begin early in nervous system development and yet deletion of Mcl-1 still results in the formation of a neural tube and primitive nervous system. Future experiments are needed to spatially resolve the expression of Mcl-1 in the nervous system and more clearly determine the extent of the deletion of Mcl-1 in the Mcl-1 CKO. Although the compensatory roles between Bcl-xL and Mcl-1 have been discovered in the nervous system as NPCs proliferate and differentiate, these roles occur after the neural tube forms (Fogarty et al., 2018). Thus, there may be redundancy with other anti-apoptotic proteins in the developing neural tube. The development of an effective antibody against Mcl-1 or a riboprobe for RNA *in situ* hybridization would allow for the proper spatial resolution of Mcl-1 expression in the developing nervous system.

Mcl-1 inhibits apoptosis through pro-apoptotic effector protein Bax; however, it is unclear through which mechanism this occurs. The likely candidate is pro-apoptotic Bim, as discussed above, but more work is needed to elucidate the exact pathway through which this occurs. Whether multiple BH3-only proteins are inhibited by Mcl-1 in the developing nervous system remains to be elucidated. Further, yet unknown pro-apoptotic proteins may be inhibited by Mcl-1. Although most of the cell death appears to be mediated through Bax, small regions in the brainstem and ventral thoracic spinal cord appear to undergo apoptosis in the absence of Bax. Future expression studies could determine if apoptosis is mediated by pro-apoptotic Bak in these regions.

Lastly, the successful rescue of embryonic lethality using the Mcl-1 CKO/BaxNull;floxed model provides an excellent system to understand the role that Mcl-1 plays in developmental neurogenesis. As previous research has shown that the

overexpression of Mcl-1 results in premature terminal mitosis (Hasan et al., 2013), it can be hypothesized that the deletion of Mcl-1 will result in a reduction in differentiation of NPCs in the developing brain. As neurogenesis does not begin until E11, the Mcl-1 CKO/BaxNull model, which is embryonic lethal by E13, is not effective at investigating the roles that Mcl-1 plays in differentiation. Identifying if the postnatal brain of the Mcl-1 CKO/BaxNull;floxed model has more NPCs and fewer differentiated neurons, or alternatively, if the double knockout has fewer early born neurons and more late born neurons would shed light on the role that Mcl-1 plays in cell-cycle exit and differentiation.

4-6 Conclusion

Here, the role that Mcl-1 plays in developmental neurogenesis was investigated. Two specific aims were addressed. First, the progression of apoptosis in the Mcl-1 CKO was investigated. The deletion of Mcl-1 results in apoptosis starting at E10 in the ventral forebrain and at E9 in the brainstem and spinal cord. Apoptosis in the brainstem and spinal cord progressed dorsally and caudally over time, similar to the progression of differentiation. Then, using a co-deletion model of *mcl-1* and *bax*, it was shown that Mcl-1 inhibits cell death in the developing nervous system through the inhibition of Bax. Lastly, although the Mcl-1 CKO/BaxNull co-deletion model was lethal by E13, another model, the Mcl-1 CKO/BaxNull;Floxed model, did rescue the embryonic lethality induced by Mcl-1 CKO alone.

In summary, the much of the early nervous system is dependent on Mcl-1 for survival and this is mediated largely through the inhibition of pro-apoptotic Bax. Future studies investigating the role that Mcl-1 plays in cell cycle exit are now possible due to the development of a double knockout model that rescues the cell death and embryonic lethality induced by the Mcl-1 CKO model alone.

5.0 References

Akhtar, R. S., Geng, Y., Klocke, B. J., Latham, C. B., Villunger, A., Michalak, E. M., . . . Roth, K. A. (2006). BH3-Only Proapoptotic Bcl-2 Family Members Noxa and Puma Mediate Neural Precursor Cell Death. *The Journal of Neuroscience, 26* (27), 7257-7264. doi: 10.1523/jneurosci.0196-06.2006

Akhtar, R. S., Klocke, B. J., Strasser, A., & Roth, K. A. (2008). Loss of BH3-only Protein Bim Inhibits Apoptosis of Hemopoietic Cells in the Fetal Liver and Male Germ Cells but Not Neuronal Cells in Bcl-x-deficient Mice. *Journal of Histochemistry & Cytochemistry, 56* (10), 921-927. doi: 10.1369/jhc.2008.951749

Alaynick, W. A., Jessell, T. M., & Pfaff, S. L. (2011). SnapShot: Spinal Cord Development. *Cell, 146* (1), 178-178.e171. doi: 10.1016/j.cell.2011.06.038

Annis, R. P., Swahari, V., Nakamura, A., Xie, A. X., Hammond, S. M., & Deshmukh, M. (2016). Mature neurons dynamically restrict apoptosis via redundant premitochondrial brakes. *FEBS J, 283* (24), 4569-4582. doi: 10.1111/febs.13944

Arbour, N., Vanderluit, J. L., Le Grand, J. N., Jahani-Asl, A., Ruzhynsky, V. A., Cheung, E. C., . . . Slack, R. S. (2008). Mcl-1 is a key regulator of apoptosis during CNS development and after DNA damage. *J Neurosci, 28* (24), 6068-6078. doi: 10.1523/JNEUROSCI.4940-07.2008

Arden, N., & Betenbaugh, M. J. (2004). Life and death in mammalian cell culture: strategies for apoptosis inhibition. *Trends in Biotechnology, 22*(4), 174-180. doi: https://doi.org/10.1016/j.tibtech.2004.02.004

Bérubé, N. G., Mangelsdorf, M., Jagla, M., Vanderluit, J., Garrick, D., Gibbons, R. J., . . . Picketts, D. J. (2005). The chromatin-remodeling protein ATRX is critical for neuronal survival during corticogenesis. *The Journal of Clinical Investigation, 115* (2), 258-267. doi: 10.1172/jci22329

Boatright, K. M., & Salvesen, G. S. (2003). Mechanisms of caspase activation. *Current Opinion in Cell Biology, 15* (6), 725-731. doi: https://doi.org/10.1016/j.ceb.2003.10.009

Brentnall, M., Rodriguez-Menocal, L., De Guevara, R. L., Cepero, E., & Boise, L. H. (2013). Caspase-9, caspase-3 and caspase-7 have distinct roles during intrinsic apoptosis. BMC cell biology, 14, 32-32. doi: 10.1186/1471-2121-14-32

Bursch, W., Kleine, L., & Tenniswood, M. (1990). The biochemistry of cell death by apoptosis. *Biochemistry and Cell Biology, 68* (9), 1071-1074.

Chen, C.V., Brummet, J.L., Jordan, C.L., & Breedlove, S.M. (2016) Down, But Not Out: Partial Elimination of Androgen Receptors in the Male Mouse Brain Does Not

Affect Androgenic Regulation of Anxiety or HPA Activity. *Endocrinology, 257* (2): 764-73

Chen, L., Willis, S. N., Wei, A., Smith, B. J., Fletcher, J. I., Hinds, M. G., . . . Huang, D. C. (2005). Differential targeting of prosurvival Bcl-2 proteins by their BH3-only ligands allows complementary apoptotic function. *Mol Cell, 17*(3), 393-403. doi: 10.1016/j.molcel.2004.12.030

Chittenden, T., Harrington, E. A., O'Connor, R., Flemington, C., Lutz, R. J., Evan, G. I., & Guild, B. C. (1995). Induction of apoptosis by the Bcl-2 homologue Bak. *Nature, 374*(6524), 733-736. doi: 10.1038/374733a0

Copp, A. J., Greene, N. D. E., & Murdoch, J. N. (2003). The genetic basis of mammalian neurulation. *Nature Reviews Genetics, 4*, 784. doi: 10.1038/nrg1181

Czabotar, P. E., Lessene, G., Strasser, A., & Adams, J. M. (2014). Control of apoptosis by the BCL-2 protein family: implications for physiology and therapy. *Nat Rev Mol Cell Biol, 15*(1), 49-63. doi: 10.1038/nrm3722

Dahlstrand, J., Lardelli, M., & Lendahl, U. (1995). Nestin mRNA expression correlates with the central nervous system progenitor cell state in many, but not all, regions of developing central nervous system. *Brain Res Dev Brain Res, 84*(1), 109-129.

De Biasio, A., Vrana, J. A., Zhou, P., Qian, L., Bieszczad, C. K., Braley, K. E., . . . Craig, R. W. (2007). N-terminal truncation of antiapoptotic MCL-1, but not G2/M-induced phosphorylation, is associated with stabilization and abundant expression in tumor cells. J Biol Chem, 282(33), 23919-23936. doi: 10.1074/jbc.M700938200

Deckwerth, T. L., Elliott, J. L., Knudson, C. M., Johnson, E. M., Jr., Snider, W. D., & Korsmeyer, S. J. (1996). BAX is required for neuronal death after trophic factor deprivation and during development. *Neuron, 17*(3), 401-411.

Dekkers, M. P. J., Nikoletopoulou, V., & Barde, Y.-A. (2013). Death of developing neurons: New insights and implications for connectivity. *J Cell Biol, 203*(3), 385-393. doi: 10.1083/jcb.201306136

Du, C., Fang, M., Li, Y., Li, L., & Wang, X. (2000). Smac, a mitochondrial protein that promotes cytochrome c-dependent caspase activation by eliminating IAP inhibition. *Cell, 102*(1), 33-42.

Duckett, C. S., Li, F., Wang, Y., Tomaselli, K. J., Thompson, C. B., & Armstrong, R. C. (1998). Human IAP-Like Protein Regulates Programmed Cell Death Downstream of Bcl-x and Cytochrome. *Molecular and Cellular Biology, 18* (1), 608-615. doi: 10.1128/mcb.18.1.608

Eckelman, B. P., Salvesen, G. S., & Scott, F. L. (2006). Human inhibitor of apoptosis proteins: why XIAP is the black sheep of the family. *EMBO reports, 7*(10), 988-994. doi: 10.1038/sj.embor.7400795

Farkas, L. M., & Huttner, W. B. (2008). The cell biology of neural stem and progenitor cells and its significance for their proliferation versus differentiation during mammalian brain development. *Curr Opin Cell Biol, 20*(6), 707-715. doi: 10.1016/j.ceb.2008.09.008

Fogarty, L. C., Flemmer, R. T., Geizer, B. A., Licursi, M., Karunanithy, A., Opferman, J. T., . . . Vanderluit, J. L. (2018). Mcl-1 and Bcl-xL are essential for survival of the developing nervous system. *Cell Death Differ*. doi: 10.1038/s41418-018-0225-1

Fogarty, L. C., Song, B., Suppiah, Y., Hasan, S. M. M., Martin, H. C., Hogan, S. E., . . . Vanderluit, J. L. (2016). Bcl-xL dependency coincides with the onset of neurogenesis in the developing mammalian spinal cord. *Mol Cell Neuroscie, 77*, 34-36. doi: 10.1016/j.mcn.2016.09.001

Gage, F. H. (2000). Mammalian neural stem cells. *Science, 287* (5457), 1433-1438.

Galluzzi, L., Vitale, I., Aaronson, S. A., Abrams, J. M., Adam, D., Agostinis, P., . . . Kroemer, G. (2018). Molecular mechanisms of cell death: recommendations of

the Nomenclature Committee on Cell Death 2018. *Cell Death Differ, 25*(3), 486-541. doi: 10.1038/s41418-017-0012-4

Gavathiotis, E., Reyna, D. E., Davis, M. L., Bird, G. H., & Walensky, L. D. (2010). BH3-triggered structural reorganization drives the activation of proapoptotic BAX. *Mol Cell, 40*(3), 481-492.

Geijsen, N. (2013). Primed to Perish: Heightened Mitochondrial Priming Explains hESC Apoptosis Sensitivity. *Cell Stem Cell, 13*(4), 371-372. doi: 10.1016/j.stem.2013.09.011

Germain, M., Milburn, J., & Duronio, V. (2008). MCL-1 inhibits BAX in the absence of MCL-1/BAX Interaction. *Journal of Biological Chemistry, 283*(10), 6384-6392.

Germain, M., Nguyen, A. P., Le Grand, J. N., Arbour, N., Vanderluit, J. L., Park, D. S., . . . Slack, R. S. (2011). MCL-1 is a stress sensor that regulates autophagy in a developmentally regulated manner. *EMBO J, 30*(2), 395-407. doi: 10.1038/emboj.2010.327

Giménez-Cassina, A., & Danial, N. N. (2015). Regulation of mitochondrial nutrient and energy metabolism by BCL-2 family proteins. *Trends in Endocrinology & Metabolism, 26*(4), 165-175. doi: 10.1016/j.tem.2015.02.004

Gouti, M., Metzis, V., & Briscoe, J. (2015). The route to spinal cord cell types: a tale of signals and switches. *Trends in Genetics, 31*(6), 282-289.

Green, D. R., & Llambi, F. (2015). Cell Death Signaling. *Cold Spring Harb Perspect Biol, 7*(12). doi: 10.1101/cshperspect.a006080

Harder, J. M., Ding, Q., Fernandes, K. A., Cherry, J. D., Gan, L., & Libby, R. T. (2012). BCL2L1 (BCL-X) promotes survival of adult and developing retinal ganglion cells. *Molecular and Cellular Neuroscience, 51*(1), 53-59. doi: https://doi.org/10.1016/j.mcn.2012.07.006

Hasan, S. M., Sheen, A. D., Power, A. M., Langevin, L. M., Xiong, J., Furlong, M., . . . Vanderluit, J. L. (2013). Mcl-1 regulates the terminal mitosis of neural precursor cells in the mammalian brain through p27Kip1. *Development, 140*(15), 3118-3127. doi: 10.1242/dev.090910

Hitoshi, S., Seaberg, R. M., Koscik, C., Alexson, T., Kusunoki, S., Kanazawa, I., . . . van der Kooy, D. (2004). Primitive neural stem cells from the mammalian epiblast differentiate to definitive neural stem cells under the control of Notch signaling. *Genes Dev, 18*(15), 1806-1811. doi: 10.1101/gad.1208404

Huang, C. R., & Yang-Yen, H. F. (2010). The fast-mobility isoform of mouse Mcl-1 is a mitochondrial matrix-localized protein with attenuated anti-apoptotic activity. FEBS Lett, 584(15), 3323-3330. doi: 10.1016/j.febslet.2010.07.013

Jeffers, J. R., Parganas, E., Lee, Y., Yang, C., Wang, J., Brennan, J., . . . Zambetti, G. P. (2003). Puma is an essential mediator of p53-dependent and -independent apoptotic pathways. *Cancer Cell, 4*(4), 321-328. doi: https://doi.org/10.1016/S1535-6108(03)00244-7

Kawaguchi, A., Miyata, T., Sawamoto, K., Takashita, N., Murayama, A., Akamatsu, W., . . . Okano, H. (2001). Nestin-EGFP Transgenic Mice: Visualization of the Self-Renewal and Multipotency of CNS Stem Cells. *Molecular and Cellular Neuroscience, 17*(2), 259-273. doi: https://doi.org/10.1006/mcne.2000.0925

Kerr, J. F., Wyllie, A. H., & Currie, A. R. (1972). Apoptosis: a basic biological phenomenon with wide-ranging implications in tissue kinetics. *British Journal of Cancer, 26*(4), 239-257.

Knudson, C. M., Tung, K. S. K., Tourtellotte, W. G., Brown, G. A. J., & Korsmeyer, S. J. (1995). Bax-Deficient Mice with Lymphoid Hyperplasia and Male Germ Cell Death. *Science, 270*(5233), 96-99.

Kozopas, K. M., Yang, T., Buchan, P., Zhou, P., & Craig, R. W. (1993). MCL-1, a gene expressed in programmed myeloid cell differentiation, has sequence similarity to BCL2. *Proceedings of the National Academy of Sciences of the United States of America, 90*(8), 3516-3520.

Krajewska, M., Mai, J. K., Zapata, J. M., Ashwell, K. W., Schendel, S. L., Reed, J. C., & Krajewski, S. (2002). Dynamics of expression of apoptosis-regulatory proteins Bid, Bcl-2, Bcl-X, Bax and Bak during development of murine nervous system. *Cell Death Differ, 9,* 145. doi: 10.1038/sj.cdd.4400934

Kristiansen, M., & Ham, J. (2014). Programmed cell death during neuronal development: the sympathetic neuron model. *Cell Death Differ, 21*(7), 1025.

Lavdas, A. A., Grigoriou, M., Pachnis, V., & Parnavelas, J. G. (1999). The Medial Ganglionic Eminence Gives Rise to a Population of Early Neurons in the Developing Cerebral Cortex. *The Journal of Neuroscience, 19*(18), 7881-7888. doi: 10.1523/jneurosci.19-18-07881.1999

Leonard, J. R., D'Sa, C., Cahn, B. R., Korsmeyer, S. J., & Roth, K. A. (2001). Bid regulation of neuronal apoptosis. *Brain Res Dev Brain Res, 128*(2), 187-190.

Letai, A., Bassik, M. C., Walensky, L. D., Sorcinelli, M. D., Weiler, S., & Korsmeyer, S. J. (2002). Distinct BH3 domains either sensitize or activate mitochondrial

apoptosis, serving as prototype cancer therapeutics. *Cancer Cell, 2*(3), 183-192. doi: https://doi.org/10.1016/S1535-6108(02)00127-7

Li, P., Nijhawan, D., Budihardjo, I., Srinivasula, S. M., Ahmad, M., Alnemri, E. S., & Wang, X. (1997). Cytochrome c and dATP-dependent formation of Apaf-1/caspase-9 complex initiates an apoptotic protease cascade. *Cell, 91*(4), 479-489.

Liang, H., Hippenmeyer, S., and Ghashghaei, H.T. (2012). A Nestin-cre transgenic mouse is insufficient for recombination in early embryonic neural progenitors. *Biol. Open, 1*(12), 1200-3.

Lindsten, T., Golden, J. A., Zong, W. X., Minarcik, J., Harris, M. H., & Thompson, C. B. (2003). The proapoptotic activities of Bax and Bak limit the size of the neural stem cell pool. *J Neurosci, 23*(35), 11112-11119.

Lindsten, T., Ross, A. J., King, A., Zong, W. X., Rathmell, J. C., Shiels, H. A., . . . Thompson, C. B. (2000). The combined functions of proapoptotic Bcl-2 family members bak and bax are essential for normal development of multiple tissues. *Mol Cell, 6*(6), 1389-1399.

Liu, J. C., Guan, X., Ryan, J. A., Rivera, A. G., Mock, C., Agrawal, V., . . . Lahav, G. (2013). High mitochondrial priming sensitizes hESCs to DNA-damage-induced apoptosis. *Cell Stem Cell, 13*(4), 483-491. doi: 10.1016/j.stem.2013.07.018

Liu, X., Kim, C. N., Yang, J., Jemmerson, R., & Wang, X. (1996). Induction of apoptotic program in cell-free extracts: requirement for dATP and cytochrome c. *Cell, 86*(1), 147-157.

Luhmann, H. J., Fukuda, A., & Kilb, W. (2015). Control of cortical neuronal migration by glutamate and GABA. *Frontiers in Cellular Neuroscience, 9*, 4-4.

Malone, C. D., Hasan, S. M., Roome, R. B., Xiong, J., Furlong, M., Opferman, J. T., & Vanderluit, J. L. (2012). Mcl-1 regulates the survival of adult neural precursor cells. *Mol Cell Neurosci, 49*(4), 439-447. doi: 10.1016/j.mcn.2012.02.003

McConnell, J. A. (1981). Identification of early neurons in the brainstem and spinal cord. II. An autoradiographic study in the mouse. *Journal of Comparative Neurology, 200*(2), 273-288. doi: doi:10.1002/cne.902000207

Michaelidis, T. M., Sendtner, M., Cooper, J. D., Airaksinen, M. S., Holtmann, B., Meyer, M., & Thoenen, H. (1996). Inactivation of bcl-2 Results in Progressive Degeneration of Motoneurons, Sympathetic and Sensory Neurons during Early Postnatal Development. *Neuron, 17*(1), 75-89. doi: 10.1016/s0896-6273(00)80282-2

Miyoshi, G., Butt, S. J., Takebayashi, H., & Fishell, G. (2007). Physiologically distinct temporal cohorts of cortical interneurons arise from telencephalic Olig2-

expressing precursors. *J Neurosci, 27*(29), 7786-7798. doi: 10.1523/jneurosci.1807-07.2007

Miyoshi, G., Hjerling-Leffler, J., Karayannis, T., Sousa, V. H., Butt, S. J., Battiste, J., . . . Fishell, G. (2010). Genetic fate mapping reveals that the caudal ganglionic eminence produces a large and diverse population of superficial cortical interneurons. *J Neurosci, 30*(5), 1582-1594. doi: 10.1523/jneurosci.4515-09.2010

Moldoveanu, T., Follis, A. V., Kriwacki, R. W., & Green, D. R. (2014). Many players in BCL-2 family affairs. *Trends Biochem Sci, 39*(3), 101-111. doi: https://doi.org/10.1016/j.tibs.2013.12.006

Motoyama, N., Wang, F., Roth, K. A., Sawa, H., Nakayama, K.-i., Nakayama, K., . . . Loh, D. Y. (1995). Massive cell death of immature hematopoietic cells and neurons in Bcl-x-deficient mice. *Science, 267*(5203), 1506-1510.

Nakamura, A., Swahari, V., Plestant, C., Smith, I., McCoy, E., Smith, S., . . . Deshmukh, M. (2016). Bcl-xL Is Essential for the Survival and Function of Differentiated Neurons in the Cortex That Control Complex Behaviors. *J Neurosci, 36*(20), 5448-5461. doi: 10.1523/JNEUROSCI.4247-15.2016

Ohtaka-Maruyama, C., & Okado, H. (2015). Molecular Pathways Underlying Projection Neuron Production and Migration during Cerebral Cortical Development. *Frontiers in Neuroscience, 9*(447). doi: 10.3389/fnins.2015.00447

Okamoto, T., Coultas, L., Metcalf, D., van Delft, M. F., Glaser, S. P., Takiguchi, M., . . . Huang, D. C. (2014). Enhanced stability of Mcl-1, a prosurvival Bcl2 relative, blunts stress-induced apoptosis, causes male sterility, and promotes tumorigenesis. *Proc Natl Acad Sci U S A, 111*(1), 261-266. doi: 10.1073/pnas.1321259110

Olivera-Martinez, I., Harada, H., Halley, P. A., & Storey, K. G. (2012). Loss of FGF-Dependent Mesoderm Identity and Rise of Endogenous Retinoid Signalling Determine Cessation of Body Axis Elongation. *PLOS Biology, 10*(10), e1001415. doi: 10.1371/journal.pbio.1001415

Oltval, Z. N., Milliman, C. L., & Korsmeyer, S. J. (1993). Bcl-2 heterodimerizes in vivo with a conserved homolog, Bax, that accelerates programed cell death. *Cell, 74*(4), 609-619. doi: https://doi.org/10.1016/0092-8674(93)90509-O

Opferman, J. T., Iwasaki, H., Ong, C. C., Suh, H., Mizuno, S.-i., Akashi, K., & Korsmeyer, S. (2005). Obligate Role of Anti-Apoptotic MCL-1 in the Survival of Hematopoietic Stem Cells. *Science, 307*(5712), 1101-1104.

Opferman, J. T., Letai, A., Beard, C., Sorcinelli, M. D., Ong, C. C., & Korsmeyer, S. J. (2003). Development and maintenance of B and T lymphocytes requires antiapoptotic MCL-1. *Nature, 426*, 671-676.

Perciavalle, R. M., Stewart, D. P., Koss, B., Lynch, J., Milasta, S., Bathina, M., . . . Opferman, J. T. (2012). Anti-apoptotic MCL-1 localizes to the mitochondrial matrix and couples mitochondrial fusion to respiration. Nature cell biology, 14(6), 575-583. doi: 10.1038/ncb2488

Print, C. G., Loveland, K. L., Gibson, L., Meehan, T., Stylianou, A., Wreford, N., . . . Cory, S. (1998). Apoptosis regulator bcl-w is essential for spermatogenesis but appears otherwise redundant. *Proc Natl Acad Sci U S A, 95*(21), 12424-12431.

Putcha, G. V., Harris, C. A., Moulder, K. L., Easton, R. M., Thompson, C. B., & Johnson, E. M., Jr. (2002). Intrinsic and extrinsic pathway signaling during neuronal apoptosis: lessons from the analysis of mutant mice. *J Cell Biol, 157*(3), 441-453. doi: 10.1083/jcb.200110108

Putcha, G. V., Moulder, K. L., Golden, J. P., Bouillet, P., Adams, J. A., Strasser, A., & Johnson, E. M. (2001). Induction of BIM, a proapoptotic BH3-only BCL-2 family member, is critical for neuronal apoptosis. *Neuron, 29*(3), 615-628.

Rakic, P. (1974). Neurons in rhesus monkey visual cortex: systematic relation between time of origin and eventual disposition. *Science, 183*(4123), 425-427.

Ramasamy, S., Narayanan, G., Sankaran, S., Yu, Y. H., & Ahmed, S. (2013). Neural stem cell survival factors. *Arch Biochem Biophys, 534*(1-2), 71-87. doi: 10.1016/j.abb.2013.02.004

Ranger, A. M., Zha, J., Harada, H., Datta, S. R., Danial, N. N., Gilmore, A. P., . . . Korsmeyer, S. J. (2003). Bad-deficient mice develop diffuse large B cell lymphoma. *Proceedings of the National Academy of Sciences, 100*(16), 9324-9329. doi: 10.1073/pnas.1533446100

Rechsteiner, M., & Rogers, S. W. (1996). PEST sequences and regulation by proteolysis. *Trends Biochem Sci, 21*(7), 267-271.

Ren, D., Tu, H.-C., Kim, H., Wang, G. X., Bean, G. R., Takeuchi, O., . . . Cheng, E. H.-Y. (2010). BID, BIM, and PUMA Are Essential for Activation of the BAX- and BAK-Dependent Cell Death Program. *Science, 330*(6009), 1390-1393. doi: 10.1126/science.1190217

Reynolds, B., & Weiss, S. (1992). Generation of neurons and astrocytes from isolated cells of the adult mammalian central nervous system. *Science, 255*(5052), 1707-1710. doi: 10.1126/science.1553558

Rinkenberger, J., Horning, S., Klocke, B. J., Roth, K. A., & Korsmeyer, S. J. (2000). Mcl-1 deficiency results in peri-implantation embryonic lethality. *Genes & Development, 14*(1), 23-27.

Roy, N., Deveraux, Q. L., Takahashi, R., Salvesen, G. S., & Reed, J. C. (1997). The c-IAP-1 and c-IAP-2 proteins are direct inhibitors of specific caspases. *EMBO J, 16*(23), 6914-6925. doi: 10.1093/emboj/16.23.6914

Sauer, B. (1998). Inducible gene targeting in mice using the Cre/lox system. *Methods, 14*(4), 381-392. doi: 10.1006/meth.1998.0593

Savitt, J. M., Jang, S. S., Mu, W., Dawson, V. L., & Dawson, T. M. (2005). Bcl-x Is Required for Proper Development of the Mouse Substantia Nigra. *The Journal of Neuroscience, 25*(29), 6721-6728. doi: 10.1523/jneurosci.0760-05.2005

Schenk, R. L., Tuzlak, S., Carrington, E. M., Zhan, Y., Heinzel, S., Teh, C. E., . . . Herold, M. J. (2017). Characterisation of mice lacking all functional isoforms of the pro-survival BCL-2 family member A1 reveals minor defects in the haematopoietic compartment. *Cell Death Differ, 24*(3), 534-545. doi: 10.1038/cdd.2016.156

Schindelin, J., Arganda-Carreras, I., Frise, E., Kaynig, V., Longair, M., Pietzsch, T., . . . Schmid, B. (2012). Fiji: an open-source platform for biological-image analysis. *Nature methods, 9*(7), 676.

Shalini, S., Dorstyn, L., Dawar, S., & Kumar, S. (2015). Old, new and emerging functions of caspases. *Cell Death Differ, 22*(4), 526-539. doi: 10.1038/cdd.2014.216

Shamas-Din, A., Kale, J., Leber, B., & Andrews, D. W. (2013). Mechanisms of action of Bcl-2 family proteins. *Cold Spring Harb Perspect Biol, 5*(4), a008714. doi: 10.1101/cshperspect.a008714

Shindler, K. S., Latham, C. B., & Roth, K. A. (1997). Bax deficiency prevents the increased cell death of immature neurons in bcl-x-deficient mice. *J Neurosci, 17*(9), 3112-3119.

Simões-Costa, M., & Bronner, M. E. (2015). Establishing neural crest identity: a gene regulatory recipe. *Development, 142*(2), 242-257. doi: 10.1242/dev.105445

Slee, E. A., Adrain, C., & Martin, S. J. (2001). Executioner caspase-3, -6, and -7 perform distinct, non-redundant roles during the demolition phase of apoptosis. J Biol Chem, 276(10), 7320-7326. doi: 10.1074/jbc.M008363200

Sun, W., Winseck, A., Vinsant, S., Park, O.-h., Kim, H., & Oppenheim, R. W. (2004). Programmed Cell Death of Adult-Generated Hippocampal Neurons Is Mediated by the Proapoptotic Gene Bax. *The Journal of Neuroscience, 24*(49), 11205-11213. doi: 10.1523/jneurosci.1436-04.2004

Takahashi, T., Nowakowski, R. S., & Caviness, V. S., Jr. (1995). The cell cycle of the pseudostratified ventricular epithelium of the embryonic murine cerebral wall. *J Neurosci, 15*(9), 6046-6057.

Takeuchi, O., Fisher, J., Suh, H., Harada, H., Malynn, B. A., & Korsmeyer, S. J. (2005). Essential role of BAX,BAK in B cell homeostasis and prevention of autoimmune disease. *Proc Natl Acad Sci U S A, 102*(32), 11272-11277. doi: 10.1073/pnas.0504783102

Thomas, L. W., Lam, C., & Edwards, S. W. (2010). Mcl-1; the molecular regulation of protein function. *FEBS, 584*(14), 2981-2989.

Thornberry, N. A., & Lazebnik, Y. (1998). Caspases: enemies within. *Science, 281*(5381), 1312-1316.

Tripathi, P., Koss, B., Opferman, J., & Hildeman, D. (2013). Mcl-1 antagonizes Bax/Bak to promote effector CD4+ and CD8+ T-cell responses. *Cell Death Differ, 20*(8), 998.

Tropepe, V., Hitoshi, S., Sirard, C., Mak, T. W., Rossant, J., & van der Kooy, D. (2001). Direct neural fate specification from embryonic stem cells: a primitive mammalian neural stem cell stage acquired through a default mechanism. *Neuron, 30*(1), 65-78.

Tropepe, V., Sibilia, M., Ciruna, B. G., Rossant, J., Wagner, E. F., & van der Kooy, D. (1999). Distinct Neural Stem Cells Proliferate in Response to EGF and FGF in the Developing Mouse Telencephalon. *Developmental Biology, 208*(1), 166-188. doi: https://doi.org/10.1006/dbio.1998.9192

Tsujimoto, Y., Cossman, J., Jaffe, E. S., & Croce, C. M. (1985). Involvement of the bcl-2 gene in human follicular lymphoma. *Science, 228*(4706), 1440-1443.

Turrero Garcia, M., & Harwell, C. C. (2017). Radial glia in the ventral telencephalon. *FEBS Lett, 591*(24), 3942-3959. doi: 10.1002/1873-3468.12829

Ulloa, F., & Briscoe, J. (2007). Morphogens and the Control of Cell Proliferation and Patterning in the Spinal Cord. *Cell Cycle, 6*(21), 2640-2649.

Vaux, D. L., Cory, S., & Adams, J. M. (1988). Bcl-2 gene promotes haemopoietic cell survival and cooperates with c-myc to immortalize pre-B cells. *Nature, 335*(6189), 440-442.

Veis, D. J., Sorenson, C. M., Shutter, J. R., & Korsmeyer, S. J. (1993). Bcl-2-deficient mice demonstrate fulminant lymphoid apoptosis, polycystic kidneys, and hypopigmented hair. *Cell, 75*(2), 229-240.

Vekrellis, K., McCarthy, M. J., Watson, A., Whitfield, J., Rubin, L. L., & Ham, J. (1997). Bax promotes neuronal cell death and is downregulated during the development of the nervous system. *Development, 124*(6), 1239-1249.

Verhagen, A. M., Ekert, P. G., Pakusch, M., Silke, J., Connolly, L. M., Reid, G. E., . . . Vaux, D. L. (2000). Identification of DIABLO, a mammalian protein that promotes apoptosis by binding to and antagonizing IAP proteins. *Cell, 102*(1), 43-53.

Walsh, J. G., Cullen, S. P., Sheridan, C., Lüthi, A. U., Gerner, C., & Martin, S. J. (2008). Executioner caspase-3 and caspase-7 are functionally distinct proteases. Proceedings of the National Academy of Sciences, 105(35), 12815-12819. doi: 10.1073/pnas.0707715105

White, F. A., Keller-Peck, C. R., Knudson, C. M., Korsmeyer, S. J., & Snider, W. D. (1998). Widespread elimination of naturally occurring neuronal death in Bax-deficient mice. *J Neurosci, 18*(4), 1428-1439.

White, L. D., & Barone, S., Jr. (2001). Qualitative and quantitative estimates of apoptosis from birth to senescence in the rat brain. *Cell Death Differ, 8*(4), 345-356. doi: 10.1038/sj.cdd.4400816

Willis, S. N., Fletcher, J. I., Kaufmann, T., van Delft, M. F., Chen, L., Czabotar, P. E., . . . Huang, D. C. S. (2007). Apoptosis Initiated When BH3 Ligands Engage Multiple Bcl-2 Homologs, Not Bax or Bak. *Science, 315*(5813), 856-859. doi: 10.1126/science.1133289

Wilson, V., Olivera-Martinez, I., & Storey, K. G. (2009). Stem cells, signals and vertebrate body axis extension. *Development, 136*(10), 1591-1604. doi: 10.1242/dev.021246

Yang, T., Kozopas, K. M., & Craig, R. W. (1995). The intracellular distribution and pattern of expression of Mcl-1 overlap with, but are not identical to, those of Bcl-2. *J Cell Biol, 128*(6), 1173-1184.

Yeo, W., & Gautier, J. (2004). Early neural cell death: dying to become neurons. *Developmental Biology, 274*(2), 233-244. doi: https://doi.org/10.1016/j.ydbio.2004.07.026

Youle, R. J., & Strasser, A. (2008). The BCL-2 protein family: opposing activities that mediate cell death. *Nat Rev Mol Cell Biol, 9*(1), 47-59.

Yuan, J., & Yankner, B. A. (2000). Apoptosis in the nervous system. *Nature, 407*, 802. doi: 10.1038/35037739

Zheng, L., Anderson, R. E., Agbaga, M.-P., Rucker, I. I. I. E. B., & Le, Y.-Z. (2006). Loss of BCL-XL in Rod Photoreceptors: Increased Susceptibility to Bright Light Stress. *Investigative Ophthalmology & Visual Science, 47*(12), 5583-5589. doi: 10.1167/iovs.06-0163

6.0 Appendix A

Table 6.1: Probability of each genetic cross when breeding to obtain an Mcl-1 CKO.

Cross:	♂ Nes:Cre$^{+/-}$ Mcl-1$^{+/-}$	X	♀ Mcl-1$^{-/-}$
Probability	**Phenotype**		**Genotype**
1/4	Mcl-1 CKO		Nes:Cre$^{+/-}$ Mcl-1$^{-/-}$
1/4	Mcl-1 Het		Nes:Cre$^{+/-}$ Mcl-1$^{+/-}$
1/2	Ctl		Mcl-1$^{-/-}$
			Mcl-1$^{+/-}$

Table 6.2: Probability of each genetic cross when breeding to obtain an Mcl-1 CKO/BaxNull.

Cross:	♂ Nes:Cre$^{+/-}$ Mcl-1$^{+/-}$ Bax$^{+/-}$	X	♀ Mcl-1$^{-/-}$ Bax$^{+/-}$
Probability	**Phenotype**		**Genotype**
1/16	Mcl-1 CKO/BaxNull		Nes:Cre$^{+/-}$ Mcl-1$^{-/-}$ Bax$^{-/-}$
1/8	Mcl-1 CKO/BaxHet		Nes:Cre$^{+/-}$ Mcl-1$^{-/-}$ Bax$^{+/-}$
1/16	Mcl-1 Het/BaxNull		Nes:Cre$^{+/-}$ Mcl-1$^{+/-}$ Bax$^{-/-}$
1/8	Mcl-1 Het/Bax Het		Nes:Cre$^{+/-}$ Mcl-1$^{+/-}$ Bax$^{+/-}$
1/16	Mcl-1 CKO		Nes:Cre$^{+/-}$ Mcl-1$^{-/-}$ Bax$^{+/+}$
1/16	Mcl-1 Het		Nes:Cre$^{+/-}$ Mcl-1$^{+/-}$ Bax$^{+/+}$
1/8	Bax Null		Mcl-1$^{+/-}$ Bax$^{-/-}$
			Mcl-1$^{-/-}$ Bax$^{-/-}$
1/4	Bax Het		Mcl-1$^{+/-}$ Bax$^{+/-}$
			Mcl-1$^{-/-}$ Bax$^{+/-}$
1/8	Ctl		Mcl-1$^{+/-}$ Bax$^{+/+}$
			Mcl-1$^{-/-}$ Bax$^{+/+}$